Frustration & Dynamics in Artificial Spin Ice

Nov. 22, 2019

Gary Wysin, Thomas Lasnier
Kansas State University
Manhattan, Kansas, U.S.A.

wysin@phys.ksu.edu
www.phys.ksu.edu/personal/wysin

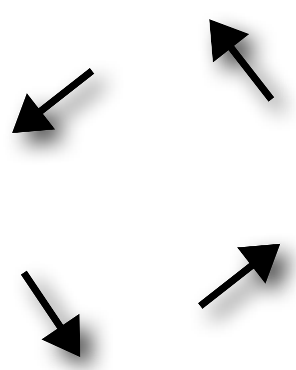

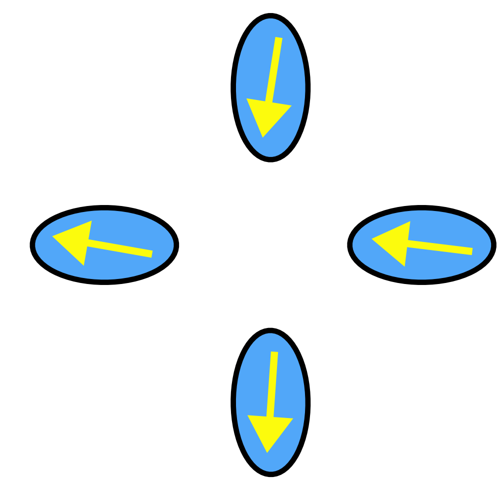

Dynamics and hysteresis in square lattice artificial spin ice

G M Wysin[1], W A Moura-Melo[2], L A S Mól[2,3,4] and A R Pereira[2]

New Journal of Physics **15** (2013) 045029 (24pp)

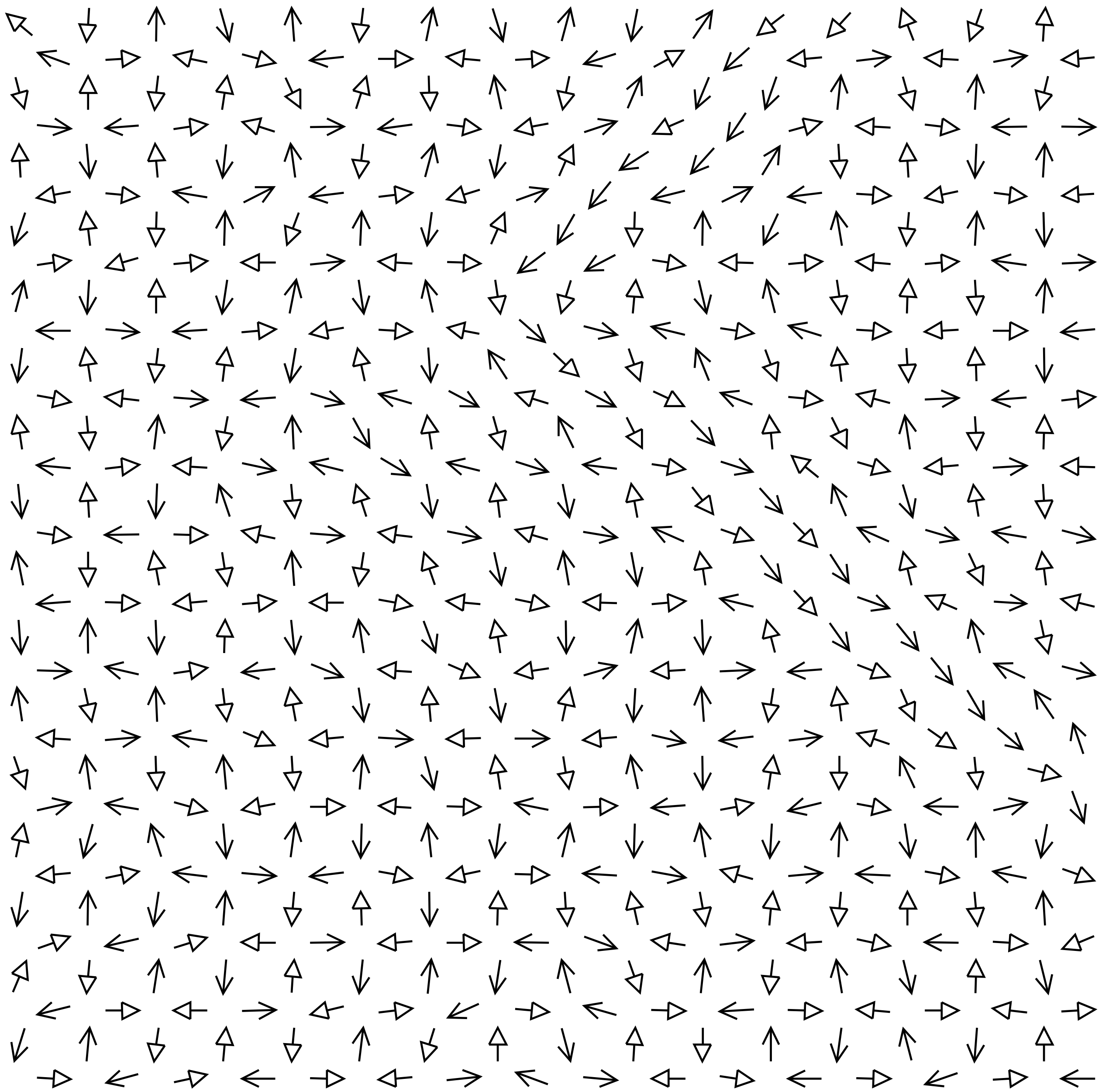

Figure 1. A 16×16 model system with $d = k_1 = k_3 = 0.1$, in a metastable state at temperature $k_B T/\varepsilon = 0.025$, from a hysteresis scan (this is a state at $h_{ext} = 0$). Most of the system is locally close to the $Z = +1$ ground state. The upper right-hand corner is locally near the $Z = -1$ ground state, and there is a bent domain wall connecting the two regions. For interior charge sites (junction points of four islands), there happens to be no discrete monopole charge present: all $q_k = 0$ and the discrete $\rho_m = 0$.

Artificial spin-ice. Arrays of elongated magnetic islands, dominated by anisotropy & dipole-dipole interactions.

Each arrow = one island.

Island rows are alternately aligned along x or y-axes in this artificial square ice.

This system has two degenerate ground states.

Mimics the behavior of 3D spin ices of rare earths in lattice of corner sharing tetrahedra of a pyrochlore structure.

in Review article: **Advances in artificial spin ice,**
Sandra Skjærvø et al. Nat. Rev. Phys. 11/08/19.

Artificial spin ices are metamaterials made up of coupled nanomagnets arranged on different lattices that exhibit a number of interesting phenomena, such as emergent magnetic monopoles, collective dynamics and phase transitions.

The ability to create thermally active artificial spin ices with fluctuating moments at room temperature makes it possible to explore the rich phase diagrams with phases that are determined by the geometry, temperature and disorder.

Signatures of the magnetic configurations are given by the specific spin-wave resonances in artificial spin ice, which offer a platform for programmable spin-wave devices, in particular magnonic crystals.

The established artificial spin ices are arranged on square and kagome lattices. New geometries include both periodic and aperiodic, different magnet shapes and anisotropies, and 3D structures.

Future work involves developments in fabrication and characterization methods, the study of artificial spin systems with new geometries and combinations of materials, and the development of applications including computation, data storage, encryption and reconfigurable microwave circuits.

Example of a rare-earth pyrochlore compound.

Pr spins at corners of tetrahedrons.

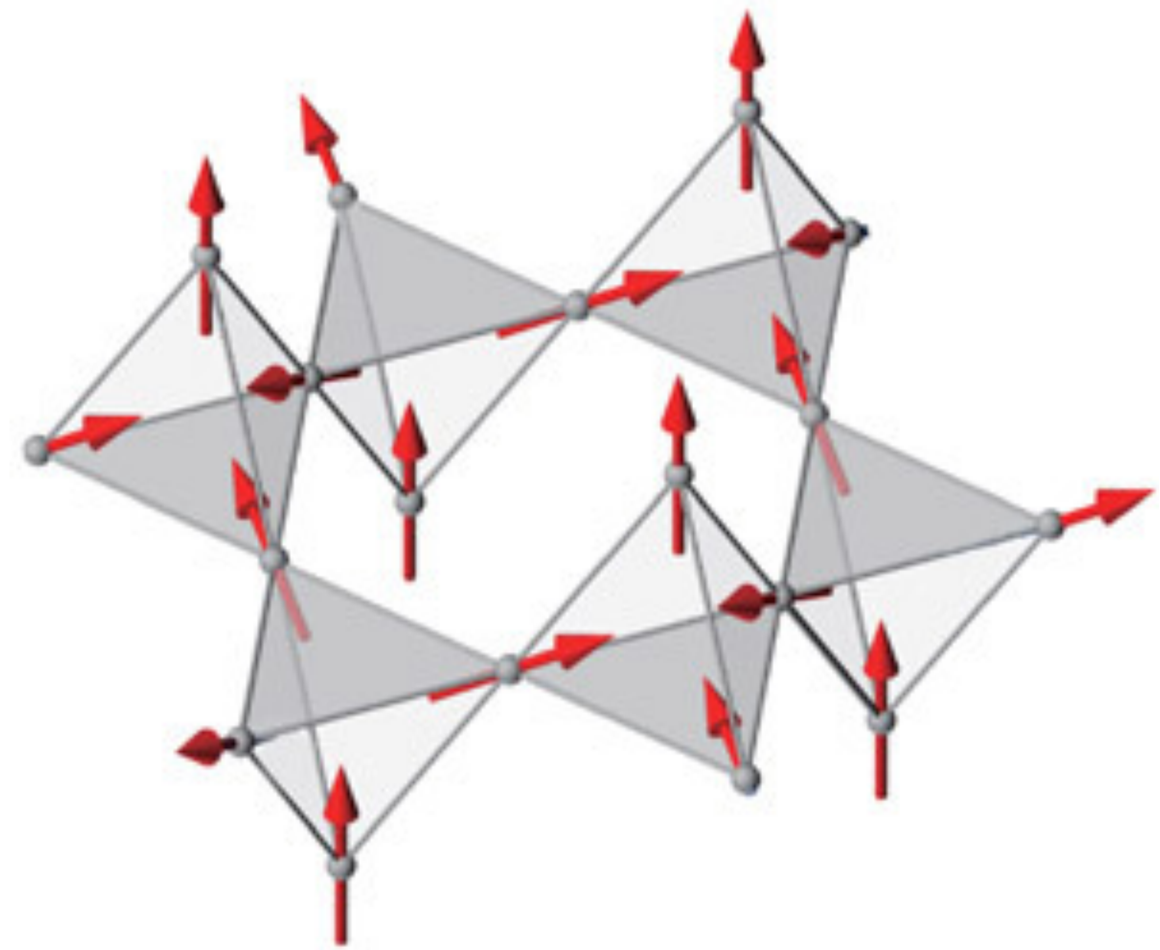

The interesting properties of $Pr_2Ir_2O_7$ are rooted in its crystal structure, called a pyrochlore lattice: four praseodymium (Pr) ions, each of which carries a magnetic ‘spin’, form a tetrahedral cage around an oxygen (O) ion. At low temperatures, the spins of materials with this structure often ‘freeze’ into what is called a ‘spin ice’ (Fig. 1) because of its similarity to the way hydrogen ions form around oxygen in water ice. (phys.org/news/)

Realization of Rectangular Artificial Spin Ice and Direct Observation of High Energy Topology

I. R. B. Ribeiro[1,6], F. S. Nascimento[2], S. O. Ferreira[1], W. A. Moura-Melo[1], C. A. R. Costa[3], J. Borme[4], P. P. Freitas[4], G. M. Wysin[5], C. I. L. de Araujo[1] & A. R. Pereira[1]

Artificial spin-ice. Arrays of elongated magnetic islands, dominated by anisotropy & dipole-dipole interactions.

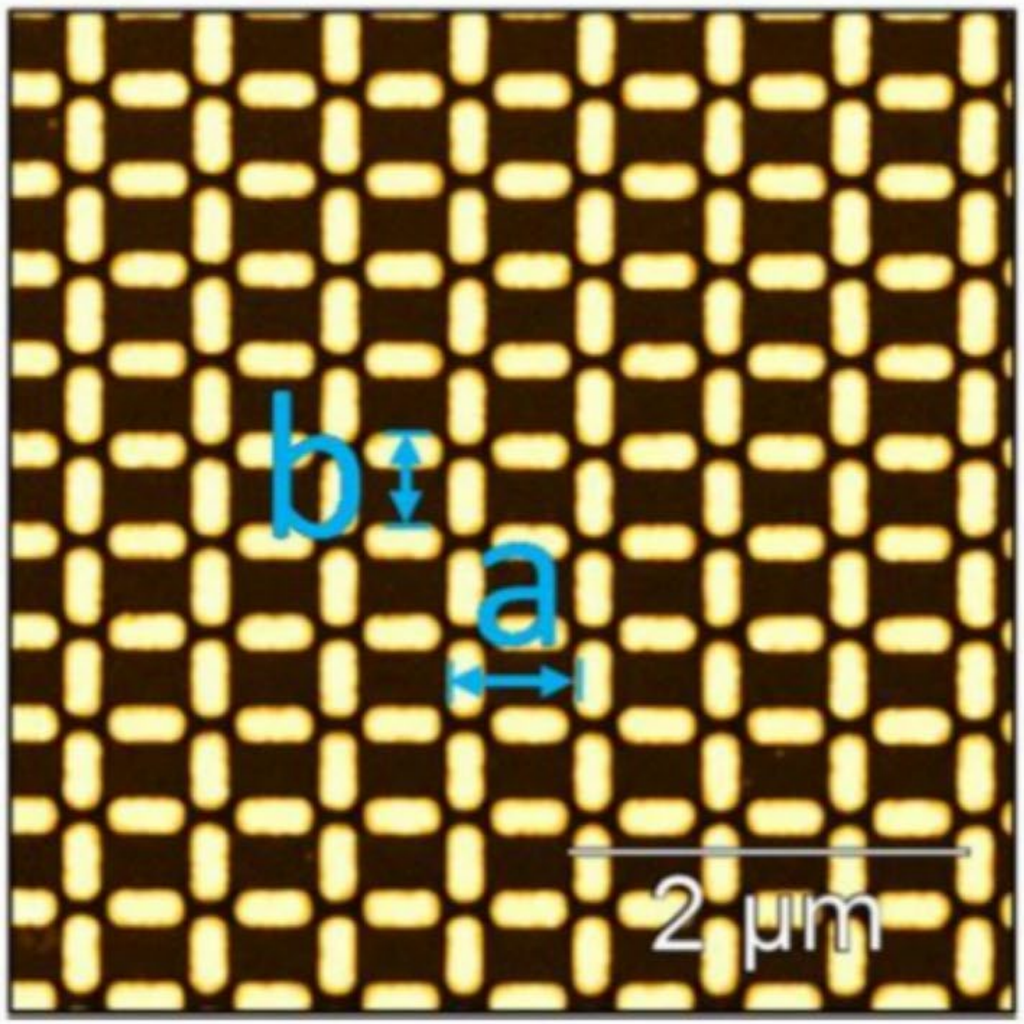

Atomic force microscope topography, 300 x 100 x 20 nm islands.

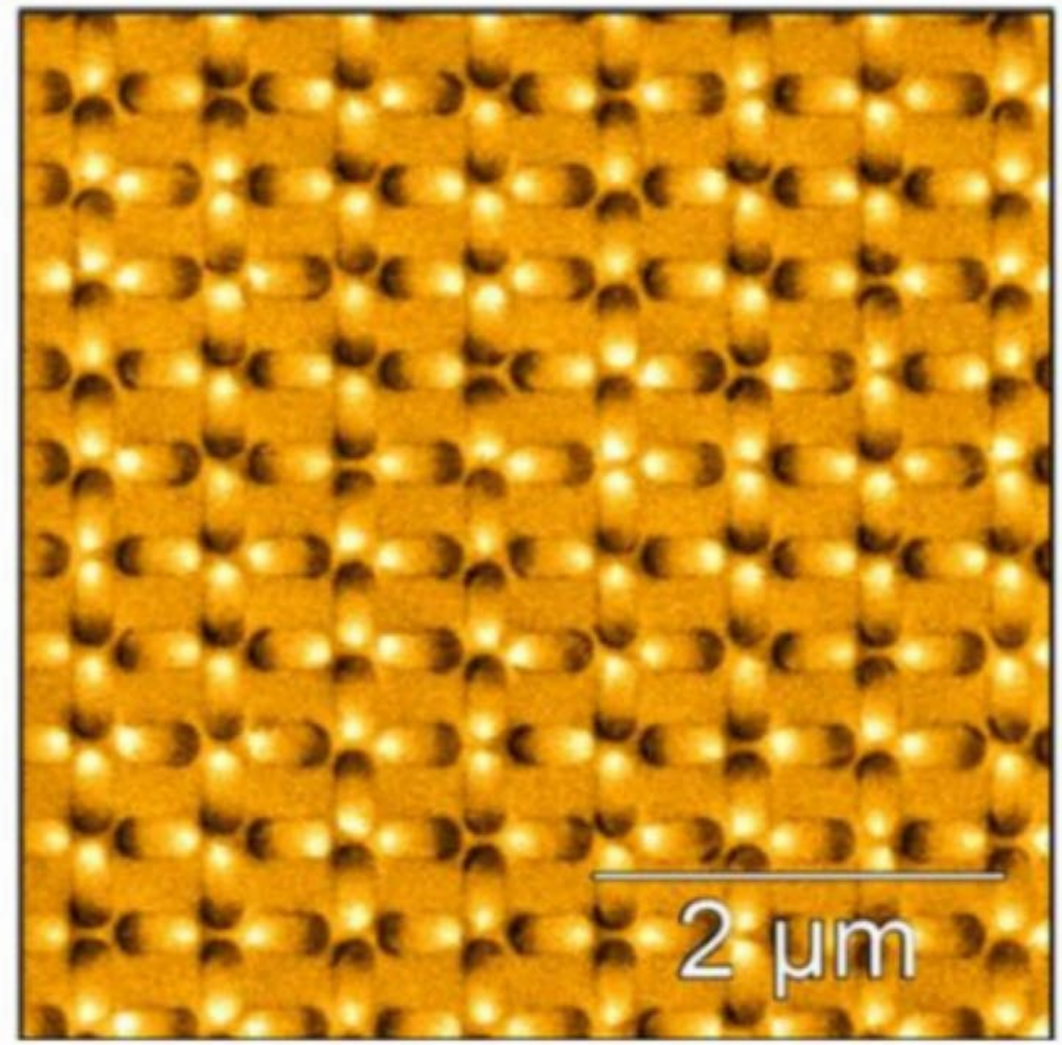

Magnetic force microscope image showing N (bright) and S (dark) poles.

Magnetic Nano-Islands
(elements of artificial spin-ice)

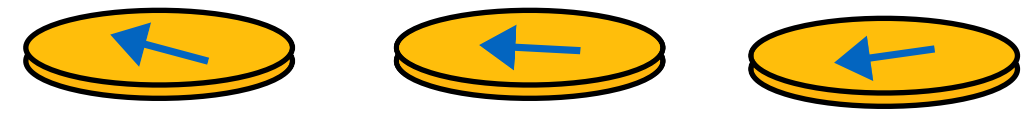

Approx. 50 nm - 5 μm wide but only 10 nm thick.
Individual & in arrays, high-permeability soft magnetic materials.
Grown with techniques of epitaxy & lithography on a non-magnetic substrate.
Form arrays of particles that can interact with each other or applied fields.

Primary physics effects -

magnetostatics controlled by island geometry.
discrete energy states for data storage.
spintronics controlled by current injection.
magnetic oscillators controlled by applied fields.
frustration in ordered arrays of islands (artificial spin-ice).

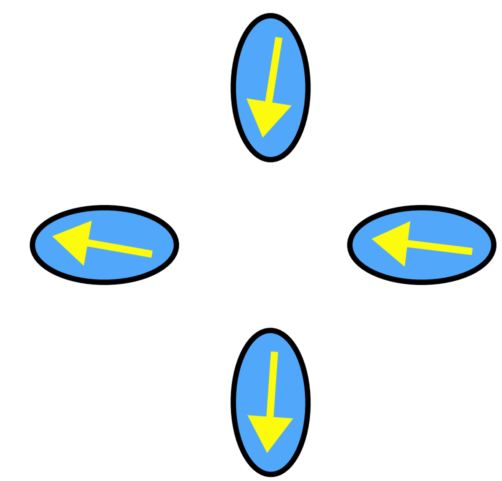

Several principle states of a nano-island:

(1) quasi-single domain; (2) vortex; (3) multi-domains & domain walls.

~ increasing size ~

Topics for study in the islands:

1) Vortices. The static and dynamic properties of single vortices. They behave very much as particles with charges.

2) Magnetostatic anisotropy of the islands themselves. Also known as shape anisotropy because it depends mostly on the surfaces.

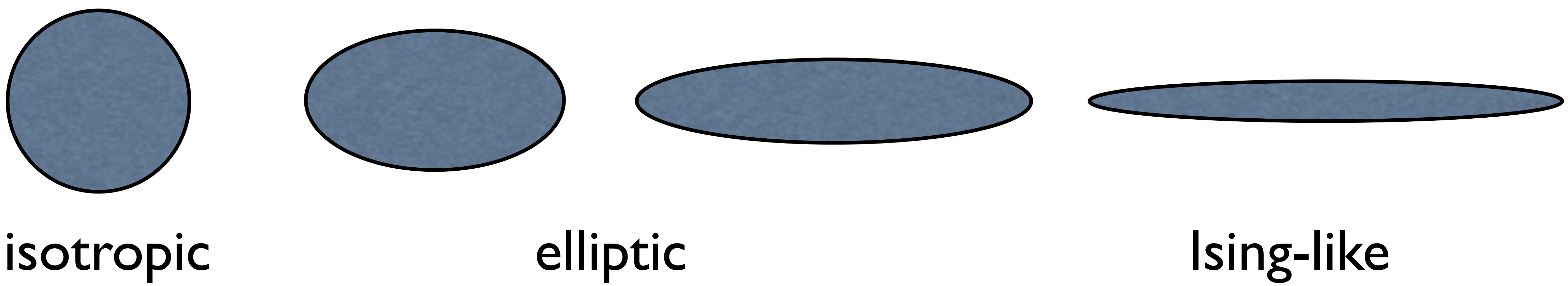

3) Spin-ices, frustration. Especially for elongated islands with Ising-like states, interactions within their arrays, that lead to frustrated statics and dynamics.

Quasi-single-domain state.

Magnetization M determines an effective surface charge density:

$$\sigma_M = \vec{M} \cdot \hat{n},$$

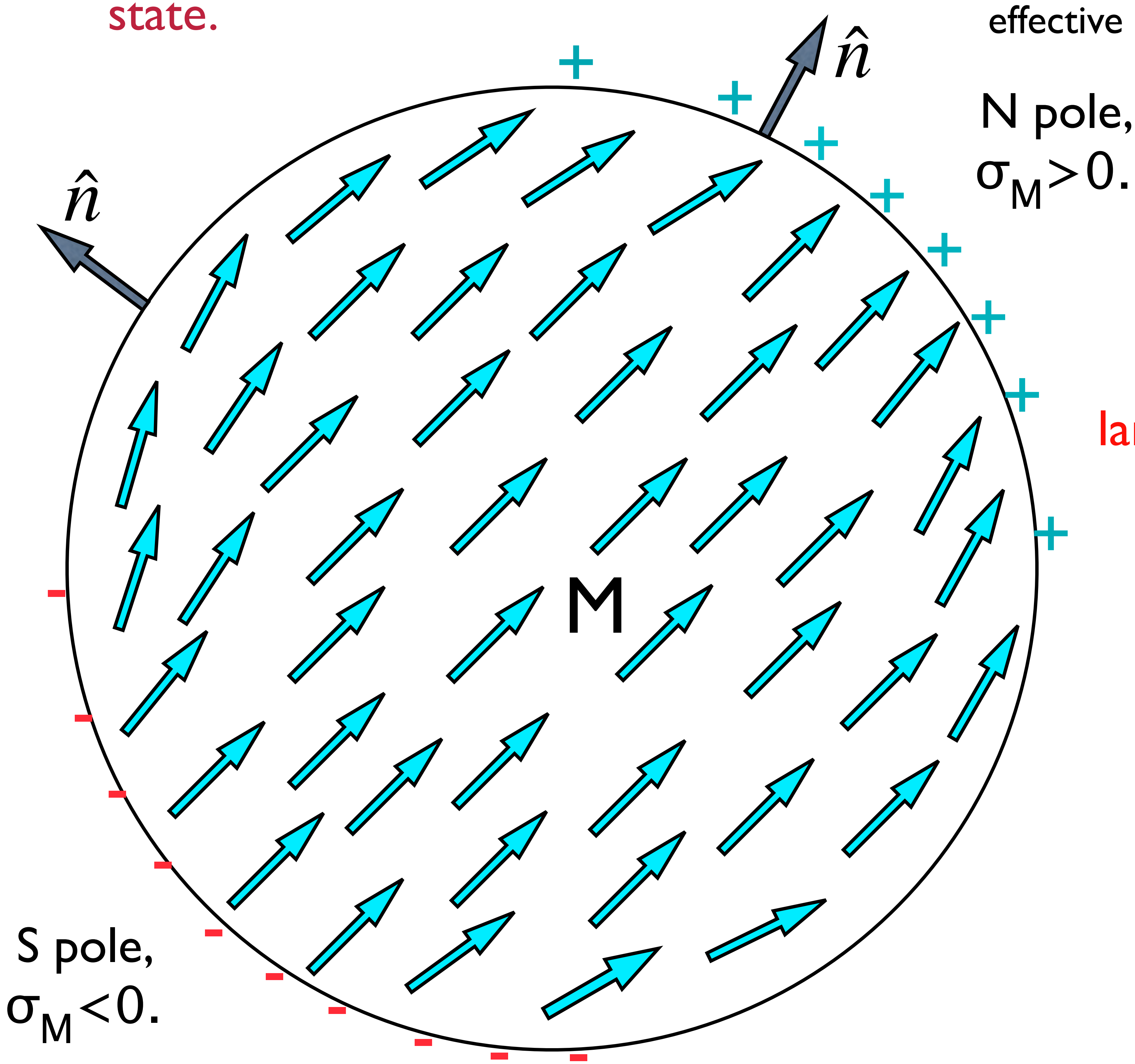

The poles produce large stray-field energy.

But ferromagnetic exchange energy is small.

Vortex state

Very little magnetic surface charge density.
Stable only above a minimum radius

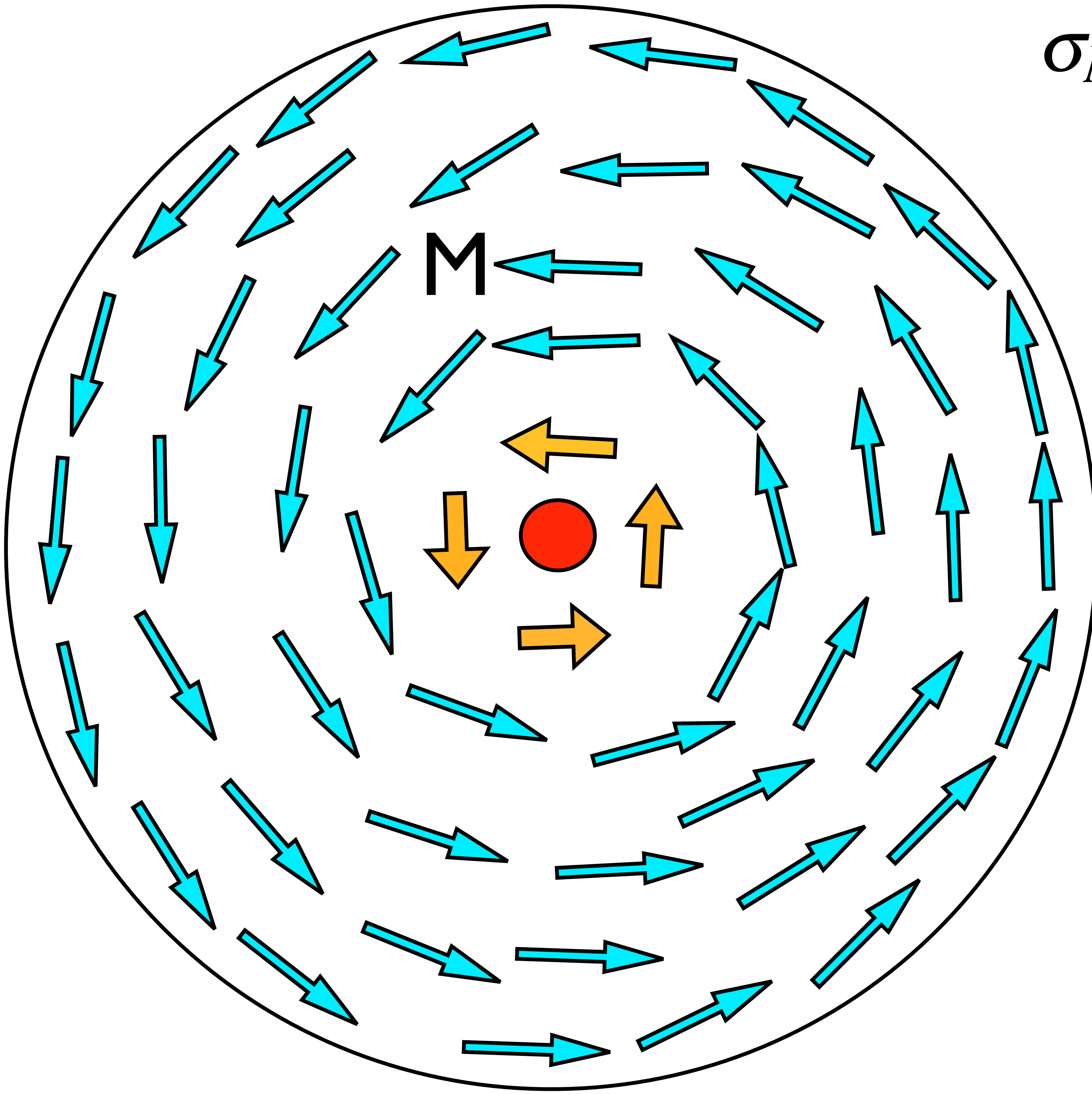

$$\sigma_M = \vec{M} \cdot \hat{n},$$

Has small poles ($\sigma_M = \pm M_z$) only in the core.

The stray-field energy is small.

But the ferromagnetic exchange energy is large.

Elongated islands -
Highly anisotropic.

Ising-like interaction
and behavior.

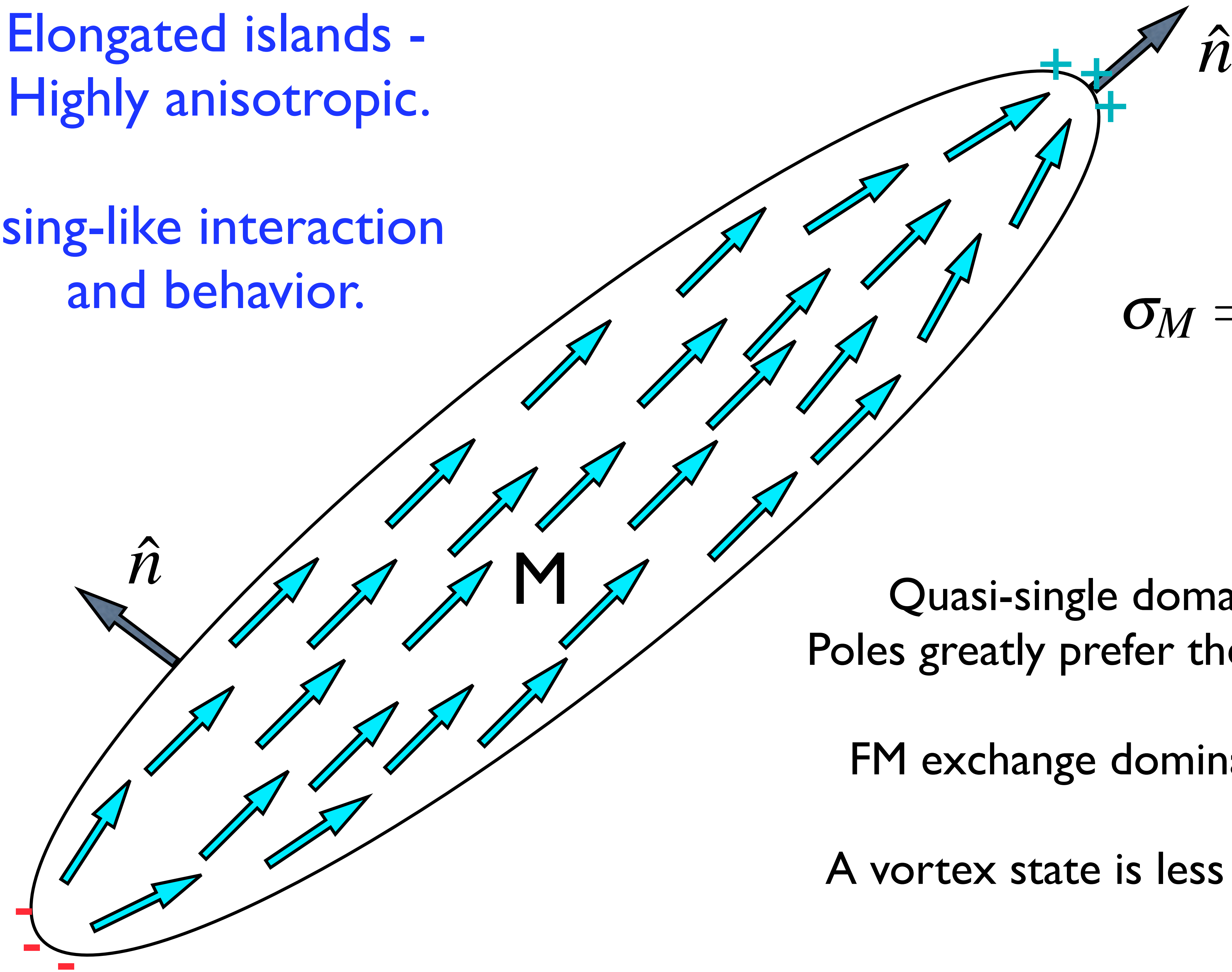

$$\sigma_M = \vec{M} \cdot \hat{n},$$

Quasi-single domain.
Poles greatly prefer the ends.

FM exchange dominates.

A vortex state is less likely.

Micromagnetics. A technique for studying a continuous system.

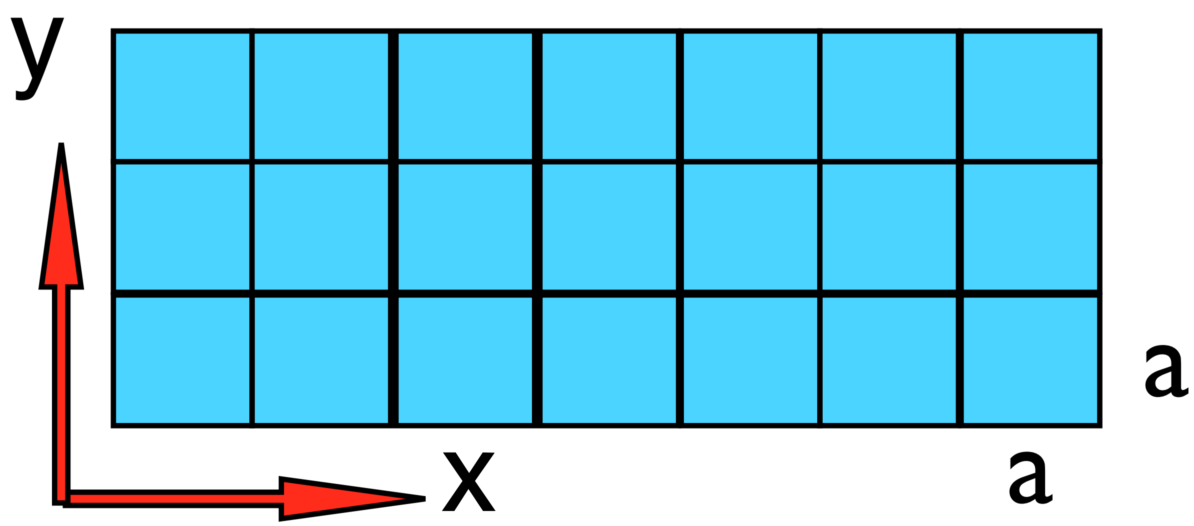

Each cell contains a magnetic dipole:

$$\hat{m} = \vec{M}/M_S.$$

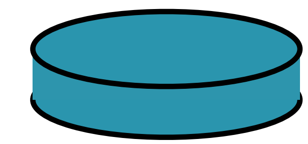

- ▶ Model for cylindrical islands, radii R_A, R_B, height L.

- ▶ Divide the sample into cells of size a x a x L.

- ▶ Assume that the magnetization is saturated (M_S) inside each cell: $|m|=1$. Only the directions vary between cells.

- ▶ The cells interact as dipoles, with exchange energy between neighbors & with the demagnetization field.

Micromagnetics

Hamiltonian: $\boxed{H = H_{ex} + H_{demag} + H_B}$

exchange:
$$\mathcal{H}_{\rm ex} = A \int dV \ \nabla \hat{m} \cdot \nabla \hat{m},$$

magnetostatic (demagnetization):
$$\mathcal{H}_{\rm dd} = \mathcal{H}_{\rm demag} = -\frac{1}{2}\mu_0 \int \ dV \ \vec{H}_M \cdot \vec{M}$$

applied field:
$$\mathcal{H}_B = -\mu_0 \int \ dV \ \vec{H}_{\rm ext} \cdot \vec{M}$$

Statics: minimize the energy $\Rightarrow$ stable configurations.
Dynamics: equation of motion $\Rightarrow$ periodic configurations.

Difficulties:

(i) Calculating the demagnetization field H_M;

(ii) Enforcing a desired initial position, X, of a vortex $\Rightarrow$ E(X).

Scale energies by the exchange between cells:

$$J_{\text{cell}} = \frac{2Av_{\text{cell}}}{a^2} = 2AL.$$

"magnetic exchange length"

$$\lambda_{\text{ex}} = \sqrt{\frac{2A}{\mu_0 M_S^2}}$$

demag. field:

$$\vec{H}_M = M_S \tilde{H}_M$$

Hamiltonian on the grid of cells:

$$\mathcal{H}_{\text{mm}} = -J_{\text{cell}} \left\{ \sum_{(i,j)} \hat{m}_i \cdot \hat{m}_j + \left(\frac{a}{\lambda_{\text{ex}}}\right)^2 \sum_i \left(\tilde{H}_{\text{ext}} + \frac{1}{2}\tilde{H}_M \right) \cdot \hat{m}_i \right\}$$

Need $\left(\frac{a}{\lambda_{\text{ex}}}\right)^2$ less than 1 for reliable solutions.

(cells smaller than exchange length)

Model for magnetic anisotropy of elliptical islands.

Total magnetic dipole moment = $\vec{\mu}$. Single domain is assumed and $\vec{\mu}$ has a fixed magnitude.

$$E = E_0 + K_1[1 - (\hat{\mu}\cdot\hat{x})^2] + K_3(\hat{\mu}\cdot\hat{z})^2$$

Include also applied field energy: $-\mu * H_{ext}$

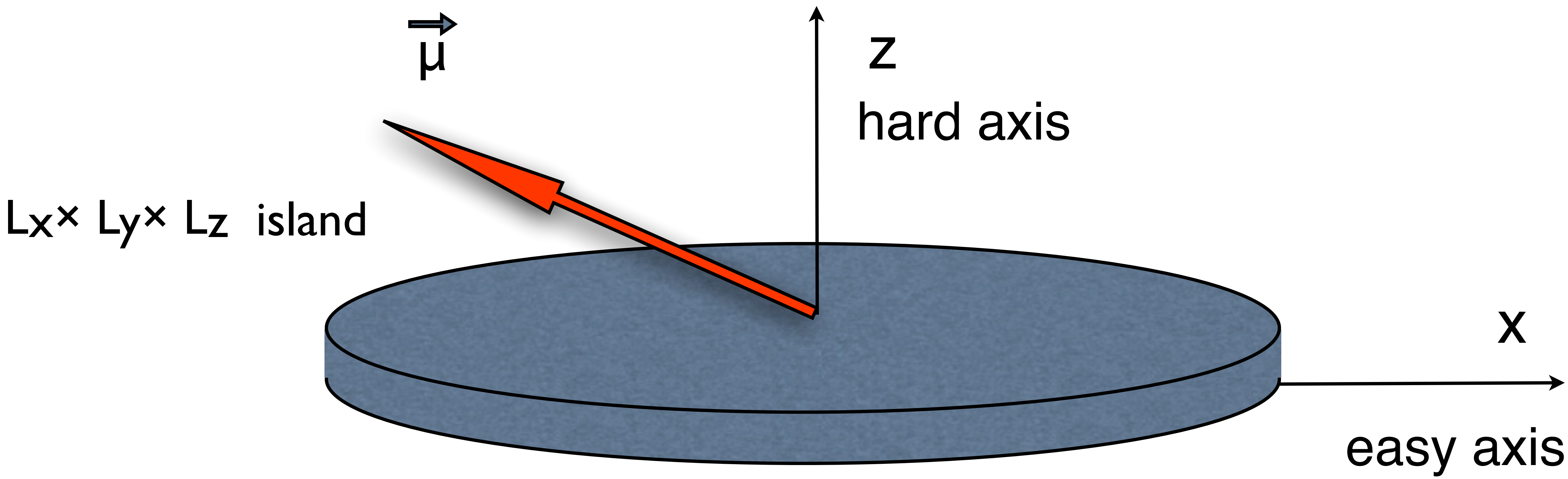

μ direction = (θ_m, ϕ_m)

angle from xy-plane

angle from x-axis

Island reversal & anisotropy

Use H_{ext} to map out the energy space of an island.
(micromagnetics in one island)

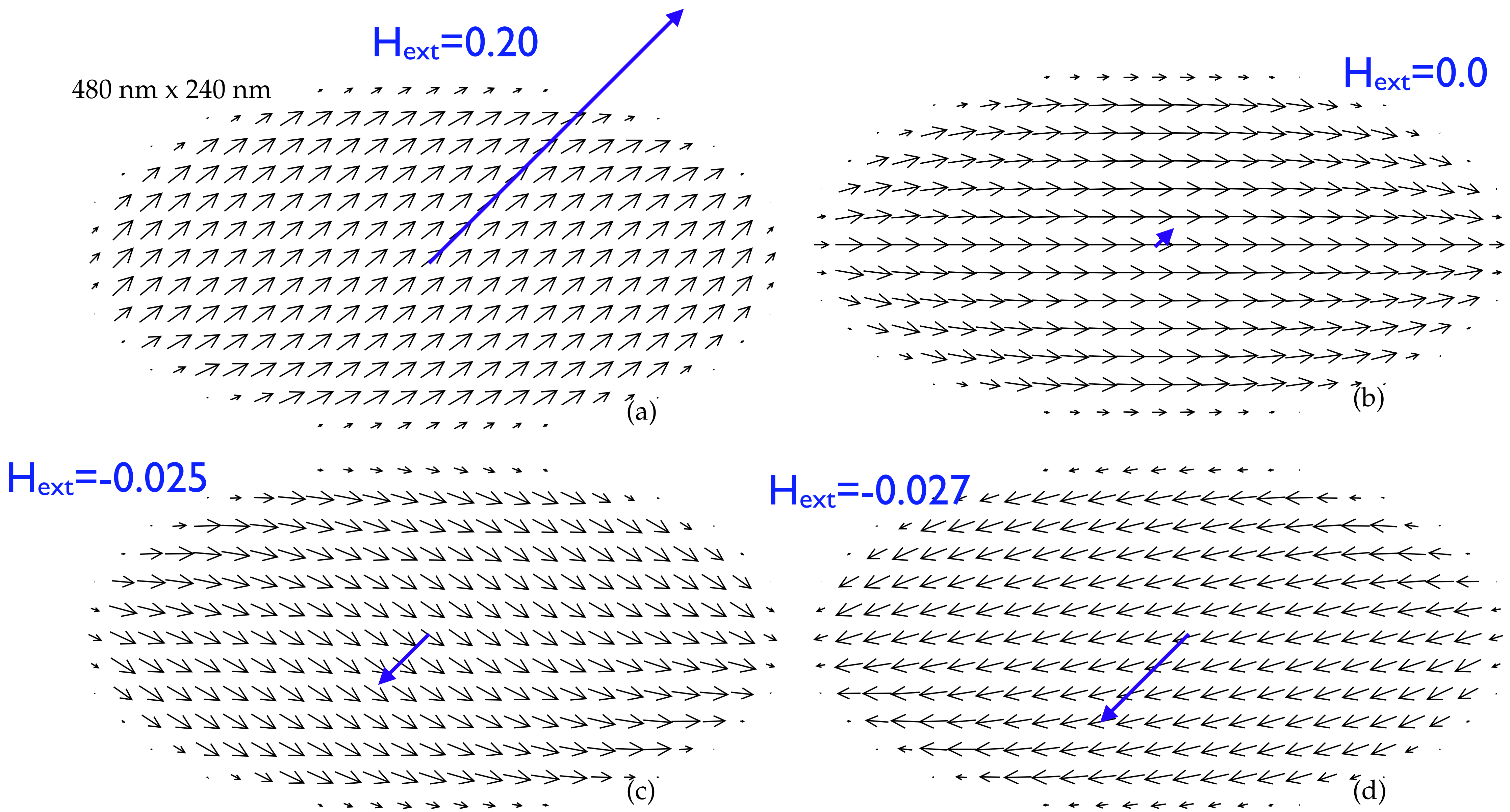

Figure 5. Magnetic configurations for a 480 nm × 240 nm × 24 nm particle with magnetic field applied at +45° above a horizontal axis pointing to the right. The arrows are the coarse-grained averages of 9 × 9 groups of cells. In (a), the external field is $h = 0.20$; in (b) $h = 0.0$; (c) $h = -0.025$, just before reversal; (d) $h = -0.027$, just after reversal. Note the enhanced curvature of the field compared to that in the smaller particle in figure 4.

internal energy

$E_{int} = E_{ex} + E_{dd}$

$$E_{\mathrm{int}}(\phi_{\mathrm{m}}) = E_0 + K_1 \sin^2\phi_{\mathrm{m}}.$$

$K_1 = 31.5\ J_{cell}$

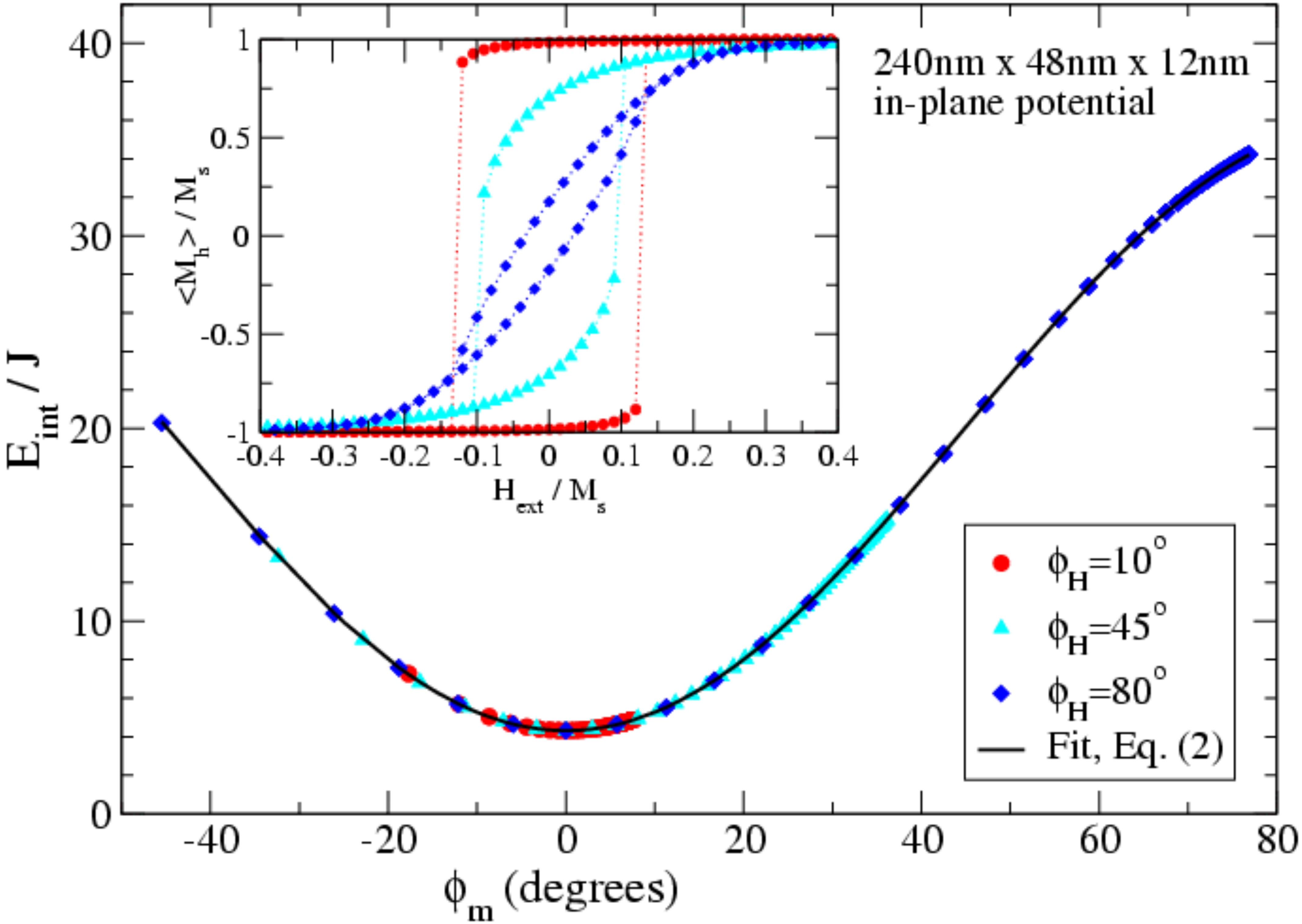

internal energy

$E_{int} = E_{ex} + E_{dd}$

$$E_{\text{int}}(\theta_{\text{m}}) = E_0 + (K_1 + K_3)\sin^2\theta_{\text{m}}. \qquad K_1+K_3=111\ J_{cell}$$

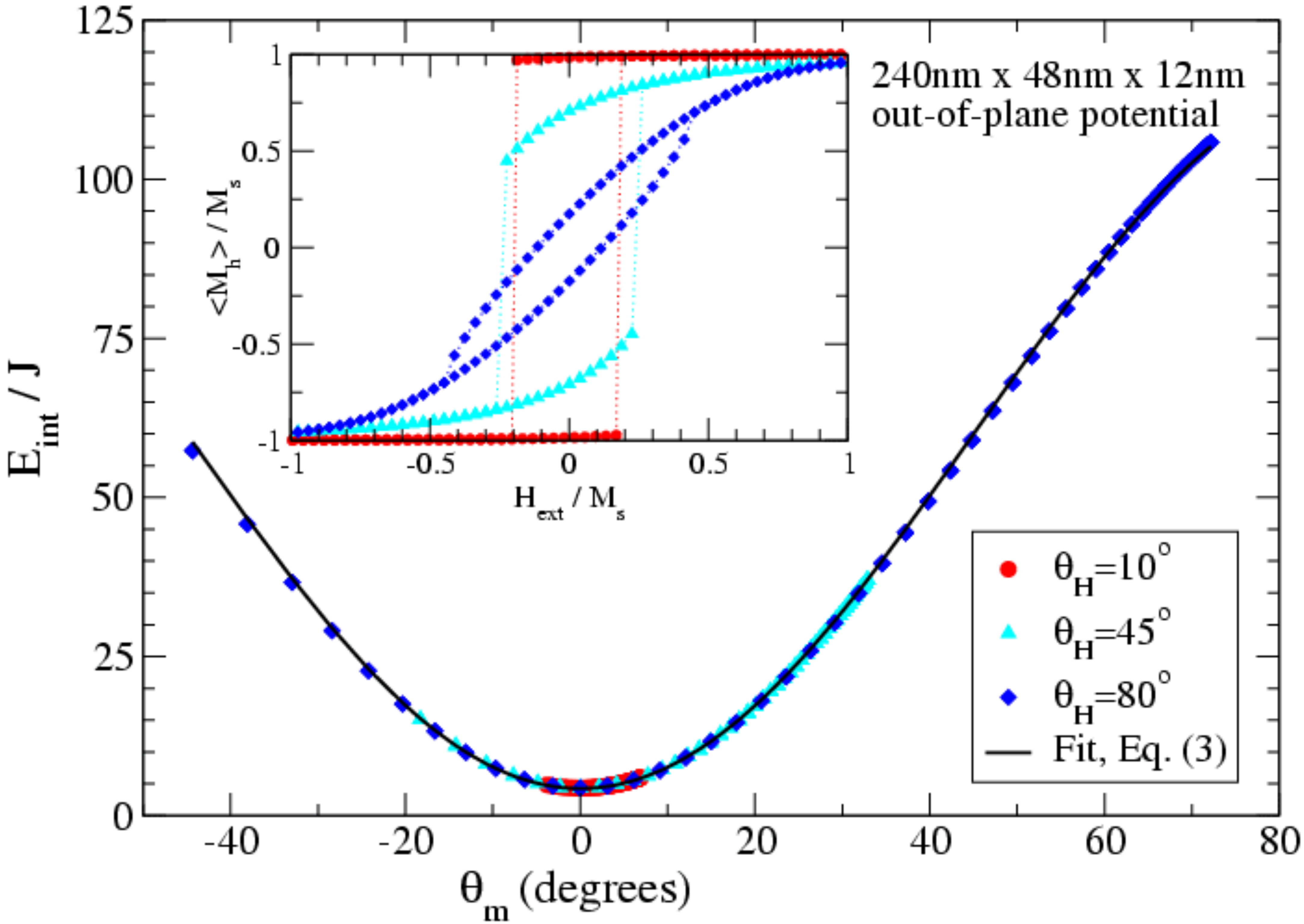

The results confirm the particle anisotropy for $L_x \times L_y \times L_z$ particles with high aspect ratios L_x/L_y:

$$\boxed{E = E_0 + K_1[1 - (\hat{\mu} \cdot \hat{x})^2] + K_3(\hat{\mu} \cdot \hat{z})^2}$$

J. Phys.: Condens. Matter **24** (2012) 296001

Table 1. Values of the in-plane anisotropy constant K_1 and out-of-plane anisotropy constant K_3 in units of $J = 2AL_z$ for different particle sizes and aspect ratios $g_1 = L_x/L_y$. All of the particles calculated have $g_3 = L_x/L_z = 20$.

	L_x					
	120 nm		240 nm		480 nm	
g_1	K_1	K_3	K_1	K_3	K_1	K_3
2	$6.35J$	$72.7J$	$27.3J$	$287J$	$111J$	$1140J$
3	$7.32J$	$43.4J$	$31.9J$	$169J$	$134J$	$670J$
5	$6.96J$	$21.1J$	$31.5J$	$79.9J$	$133J$	$311J$
8	$7.39J$	$8.30J$	$29.5J$	$33.1J$	$118J$	$132J$

Anisotropy constants per unit volume depend mainly on aspect ratios.

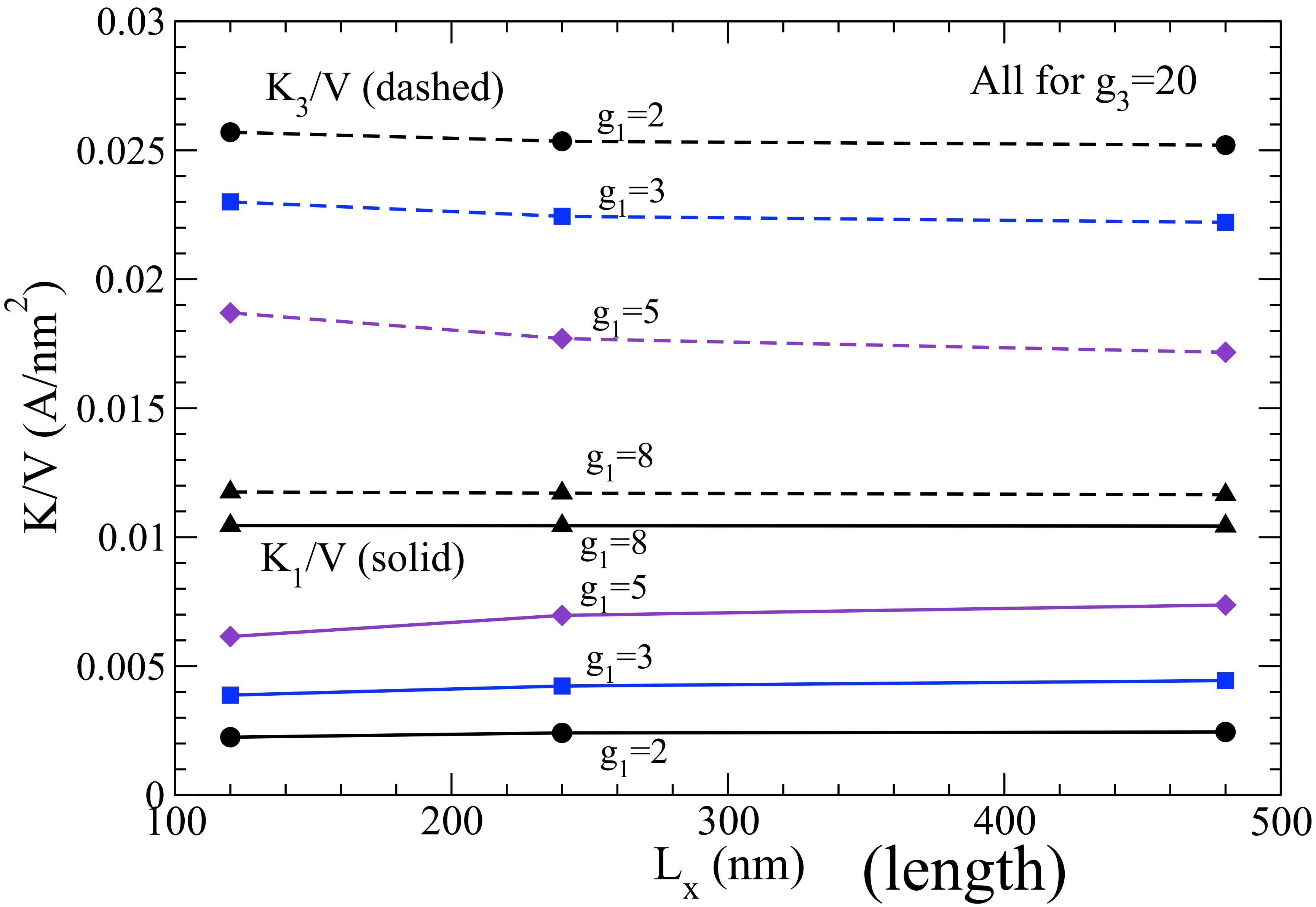

aspect ratios

$g_1 = L_x / L_y$

$g_3 = L_x / L_z$

Figure 3. The anisotropy constants K_1 (solid curves) and K_3 (dashed curves) scaled by elliptical particle volume, versus particle lengths, for the indicated g_1 aspect ratios. All data has $g_3 = 20$. The values of K/V are given in units of A nm^{-2}, where A is the exchange stiffness. K_1/V increases with aspect ratio while K_3/V decreases, and they become equal at high aspect ratio.

What is frustration?

FM on square lattice

$E_{ij} = -JS_i\,S_j$

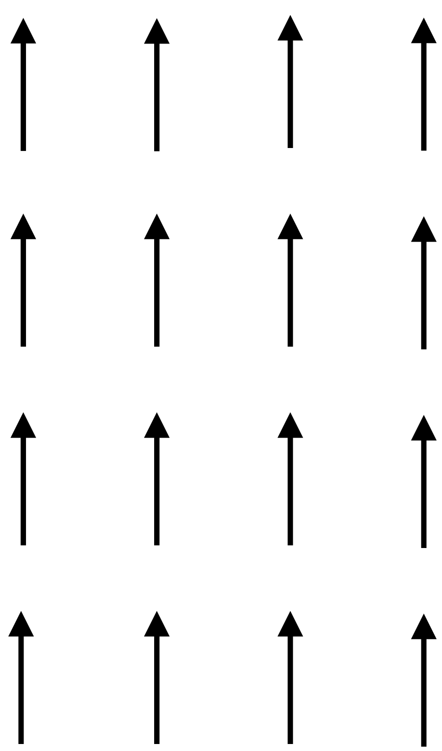

FM - unique ground state
no frustration

Anti-FM on square lattice

$E_{ij} = +JS_i\,S_j$

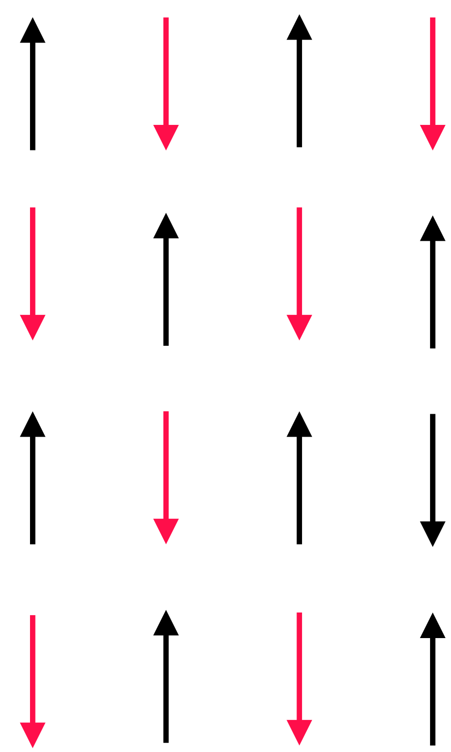

Anti-FM - 2 ground states
but still no frustration

AFM on triangular lattice

$E_{ij} = +JS_i\,S_j$

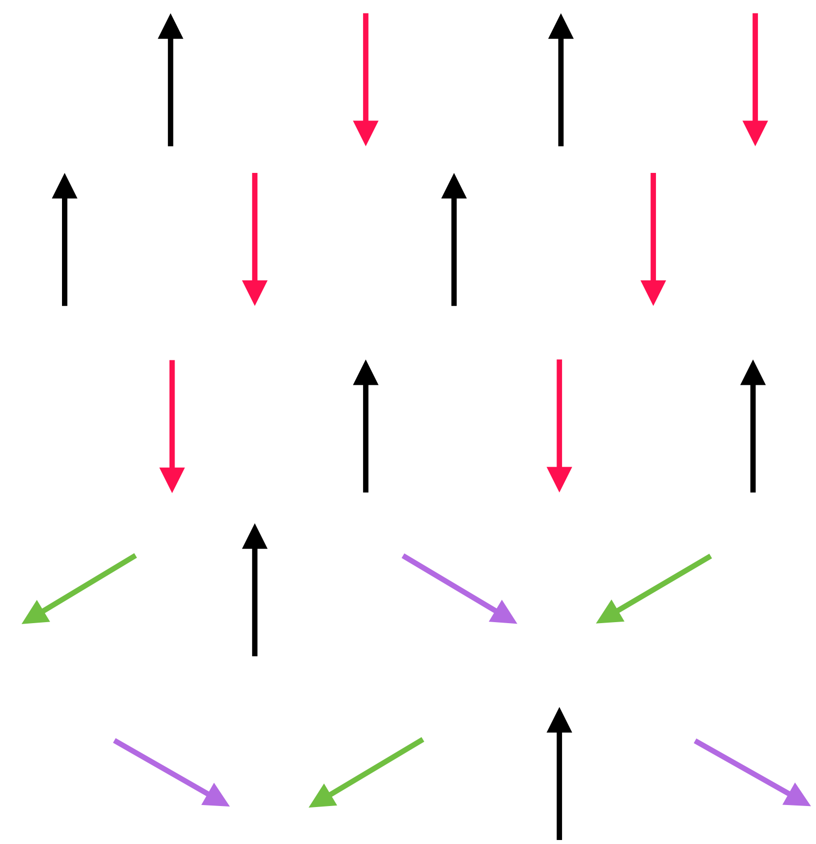

Anti-FM - multi ground states
with frustration.
Not all bond energies can
acquire their minima.

dipolar interactions

$$\mathcal{H}_{\rm dd} = -\frac{\mu_0}{4\pi}\mu_{\rm cell}^2 \sum_{i>j} \frac{[3(\hat{m}_i\cdot\hat{r}_{ij})(\hat{m}_j\cdot\hat{r}_{ij}) - \hat{m}_i\cdot\hat{m}_j]}{|\vec{r}_i-\vec{r}_j|^3}.$$

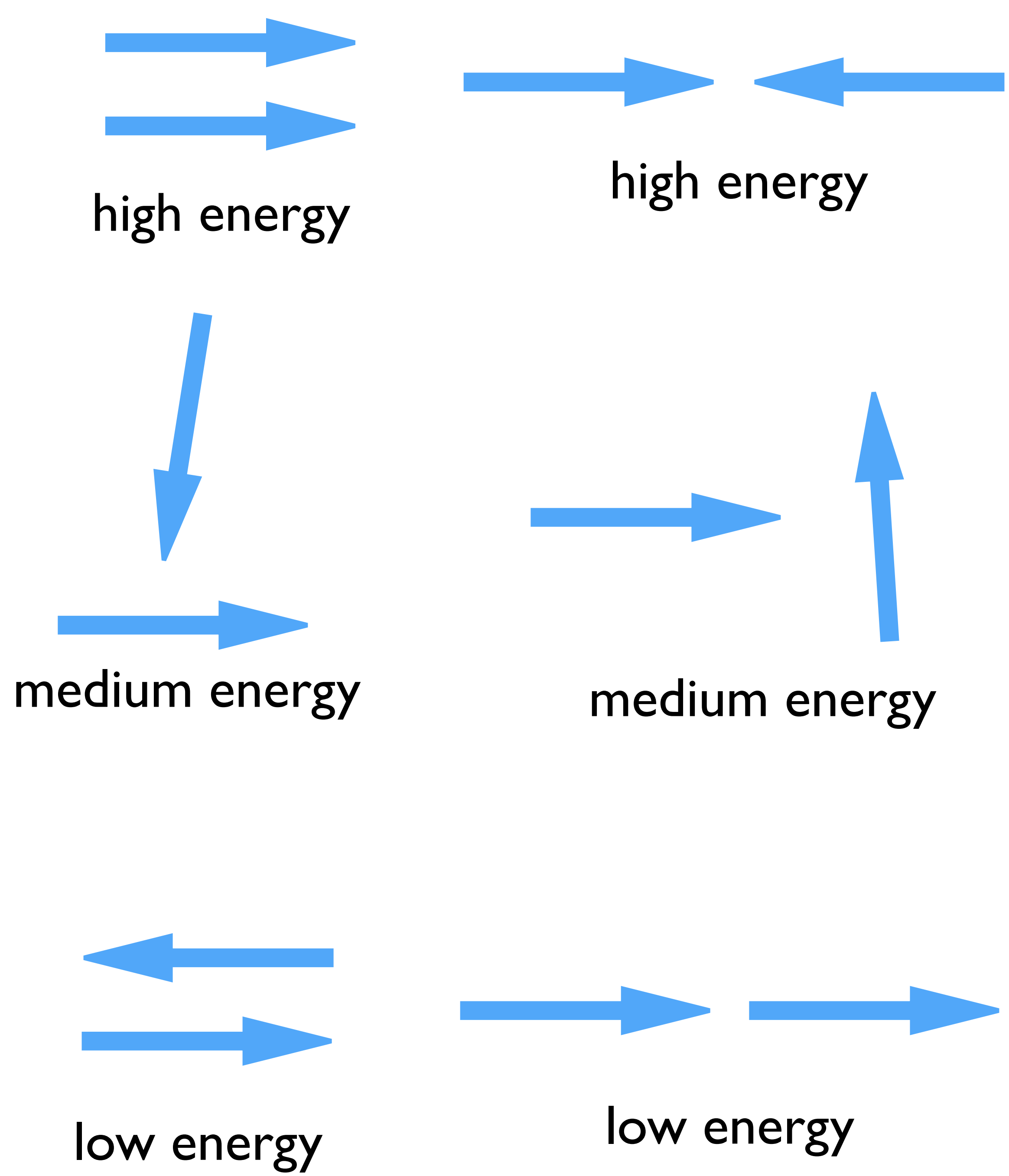

frustration in a spin-ice vertex (dipolar interactions)

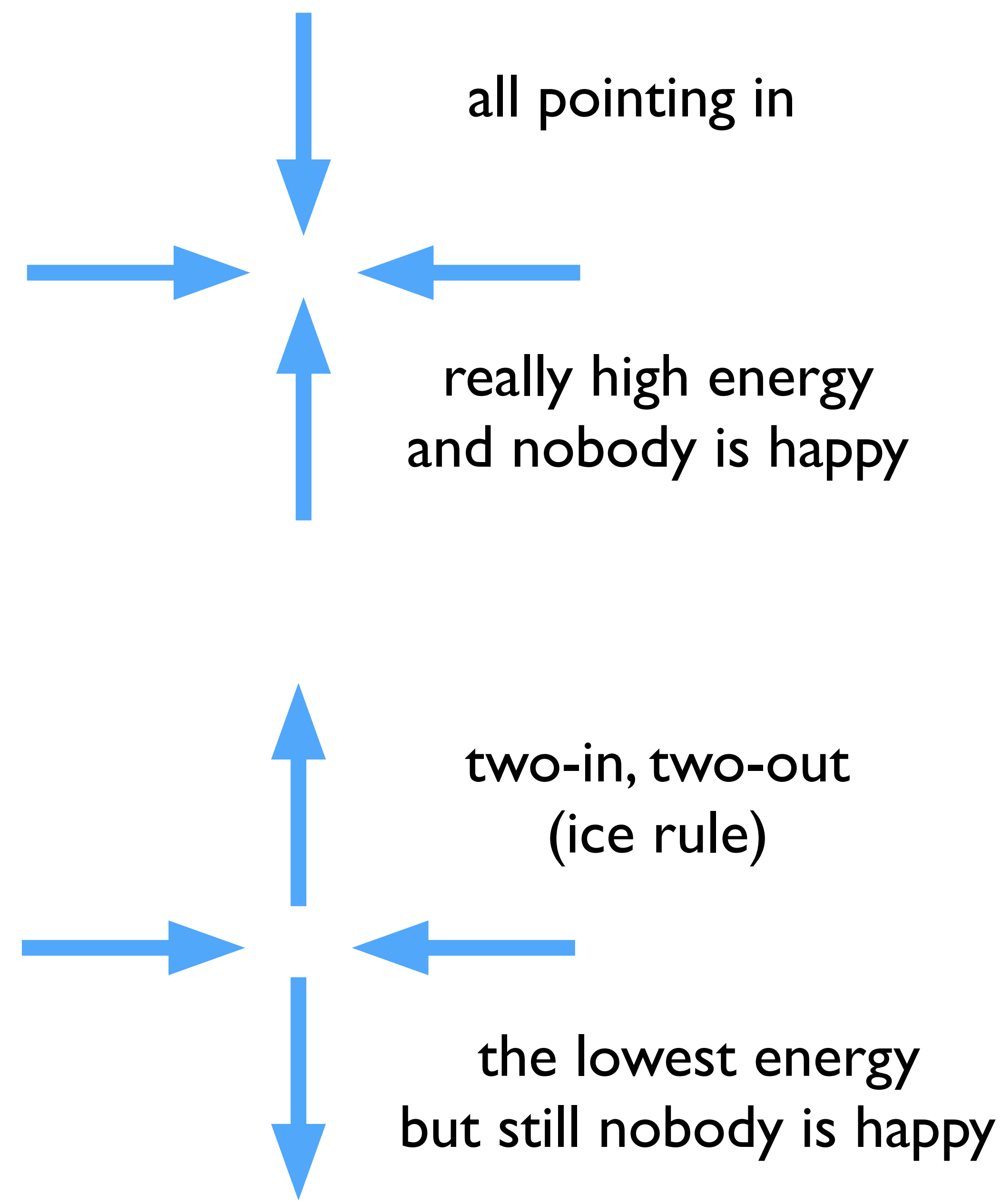

Interactions = dipolar + shape anisotropy + external field

$$\mathcal{H} = -\frac{\mu_0}{4\pi}\frac{\mu^2}{a^3}\sum_{i>j}\frac{[3(\hat{\mu}_i\cdot\hat{r}_{ij})(\hat{\mu}_j\cdot\hat{r}_{ij}) - \hat{\mu}_i\cdot\hat{\mu}_j]}{(r_{ij}/a)^3} + \sum_i\{K_1[1-(\hat{\mu}_i\cdot\hat{u}_i)^2]+K_3(\hat{\mu}_i\cdot\hat{z})^2 - \vec{\mu}_i\cdot\vec{B}_{\text{ext}}\}$$

easy axis hard axis

dipolar energy scale = D

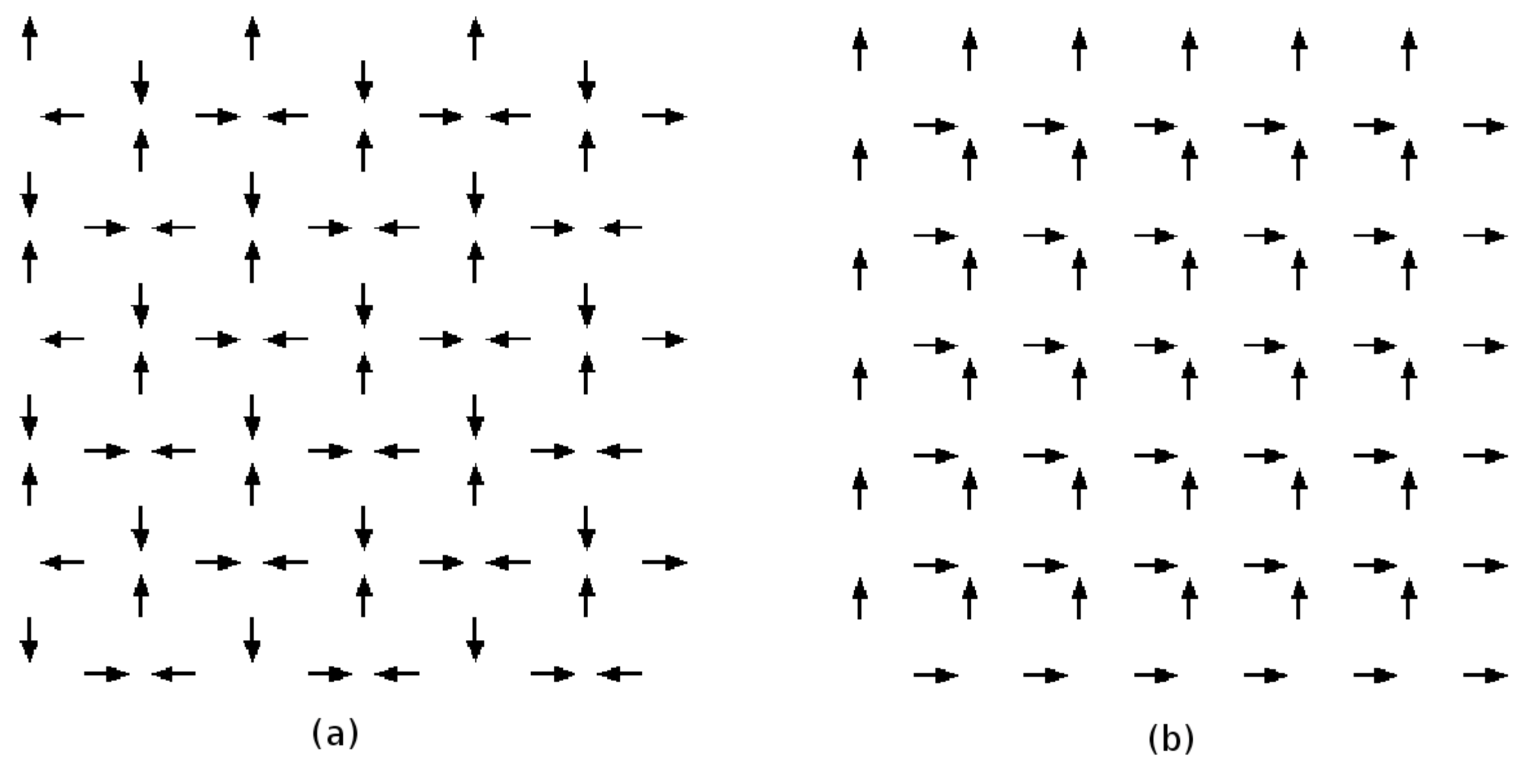

Ice-rule:

For lowest energy, equal numbers of inward and outward pointing dipoles at each vertex.

FIG. 2: (a) Configuration of the ground-state obtained for $L = 6a$, in exact agreement with that experimentally observed. Note that the ice rules are manifested at each vertex. This is the case in which the topology demands the minimum energy (see Fig. (3)). (b) Another configuration also respecting the ice rule, but displaying a topology which costs more energy. (Mol et al 2008.)

quantized excitations in a vertex

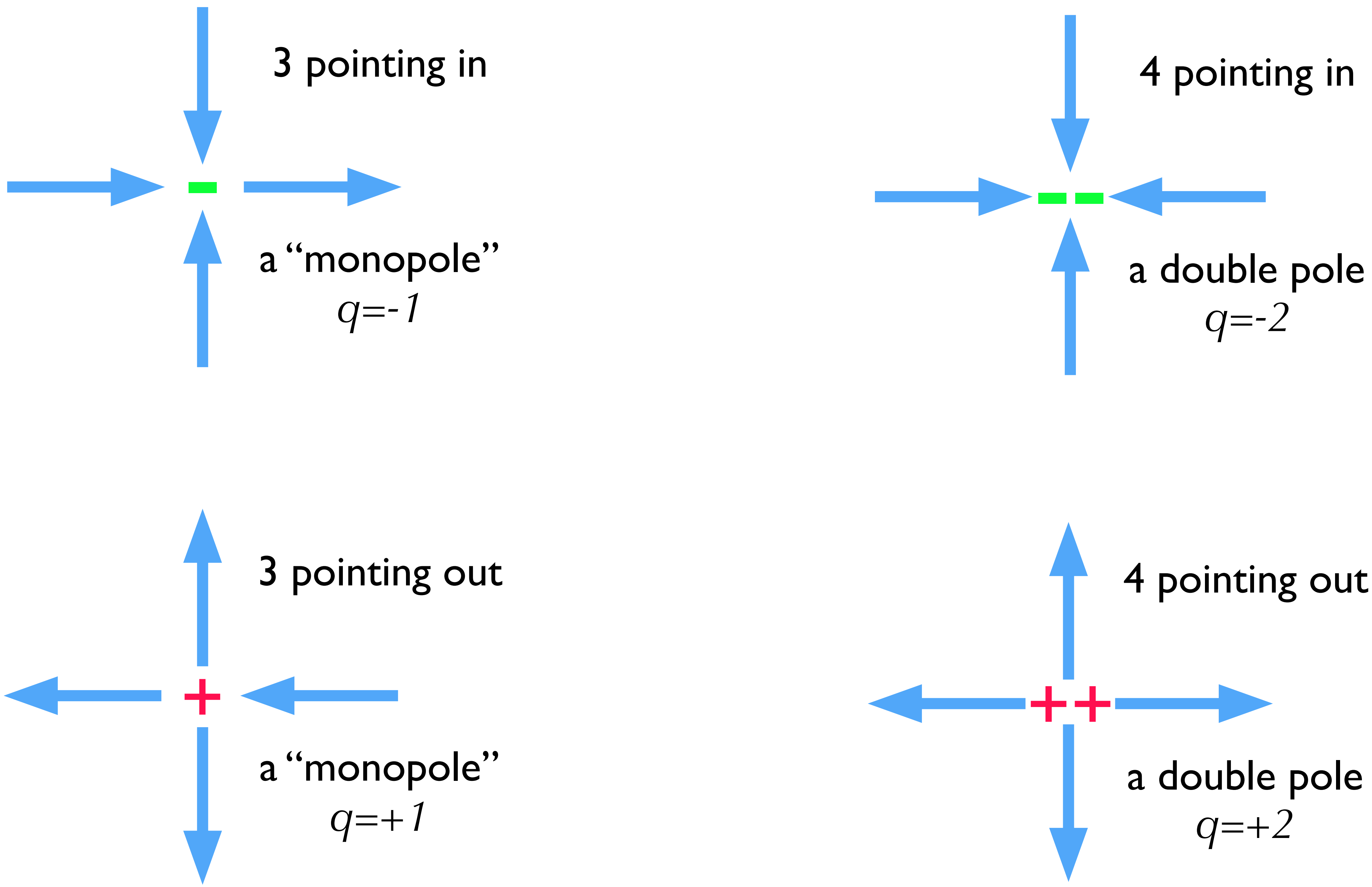

energies of Ising-like states of a vertex

Type I (2) $E_{\mathrm{I}} = -13.0D$ | Type II (4) $E_{\mathrm{II}} = -4.0D$ | Type III (8) $E_{\mathrm{III}} = 0$ | Type IV (2) $E_{\mathrm{IV}} = 21.0D$

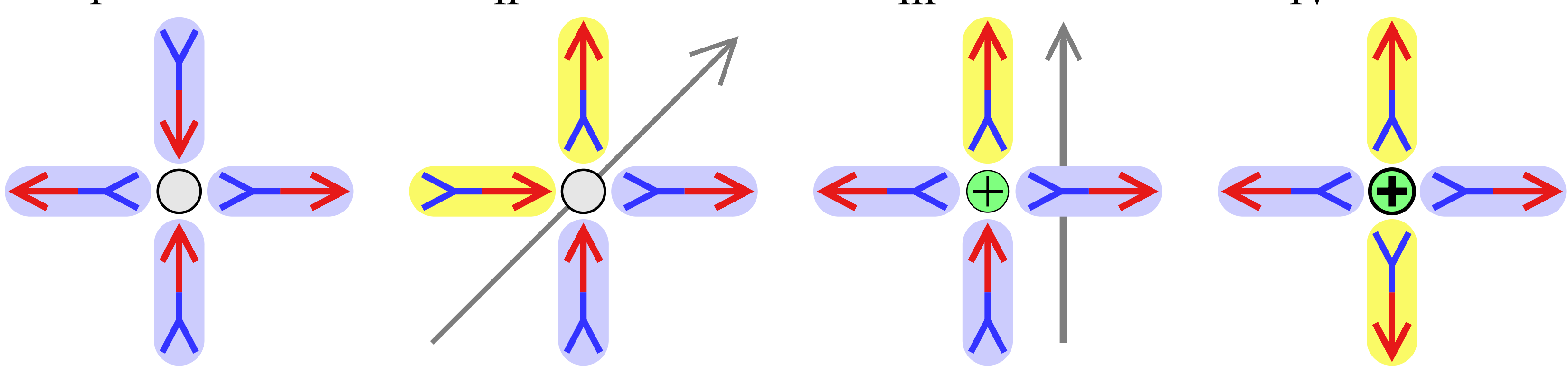

$$D \equiv \frac{\mu_0}{4\pi}\frac{\mu^2}{a^3}.$$

deviations from the ice rule
$\Rightarrow$ higher energy and monopole "charges"

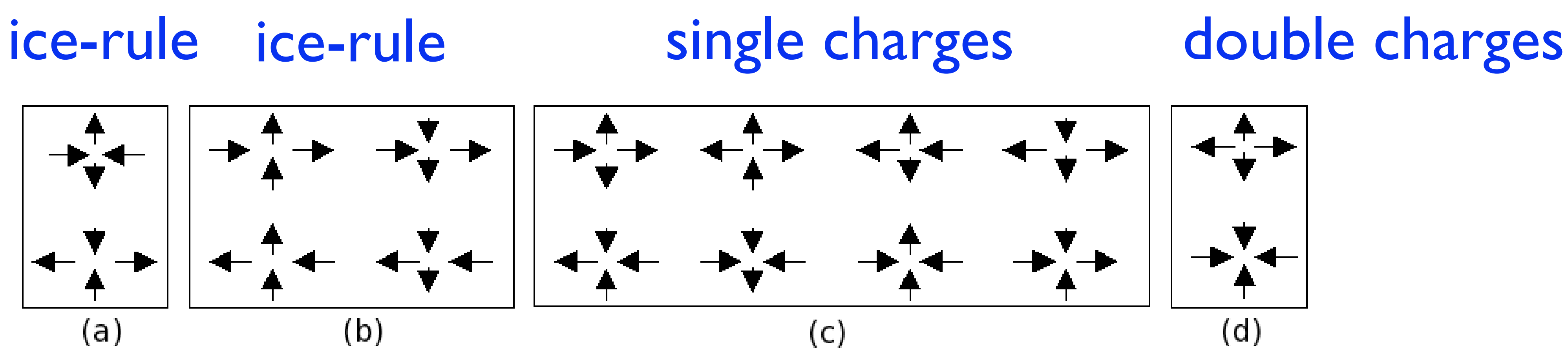

FIG. 3: The 4 distinct topologies and the 16 possible magnetic moment configurations on a vertex of 4 islands. Although configurations (a) and (b) obey the ice rule, the topology of (a) is more energetically favorable than that of (b). Hamiltonian (1) correctly yields to the true ground-state based on topology (a), without further assumptions. Topologies (c) and (d) does not obey the ice rule. Particularly, (c) implies in a monopole with charge Q_M.

How do the excitations behave as particles, interact with each other, and contribute to thermodynamics?

With temperature T>0. For the movement in one cell:

$$\boxed{\frac{d\hat{m}}{d\tau} = \hat{m} \times \left(\vec{b} + \vec{b}_s\right) - \alpha \hat{m} \times \left[\hat{m} \times \left(\vec{b} + \vec{b}_s\right)\right]}$$

stochastic fields

fluctuation-dissipation theorem:

$$\langle b_s^\alpha(\tau)\, b_s^\beta(\tau')\rangle = 2\alpha\,\mathcal{T}\,\delta_{\alpha\beta}\,\delta(\tau - \tau') \qquad \mathcal{T} \equiv \frac{kT}{J_{\text{cell}}} = \frac{kT}{2AL}$$

(the stochastic fields carry thermal energy & power)

We can integrate with Heun's 2nd order algorithm:

A. Euler predictor step.
B. Trapezoid corrector step.

$$\int_{\tau_n}^{\tau_n+\Delta\tau} d\tau\ b_s^x(\tau) \longrightarrow \sigma_s w_n^x$$

ran( )

$$\sigma_s = \sqrt{2\alpha\mathcal{T}\,\Delta\tau}.$$

artificial ice model

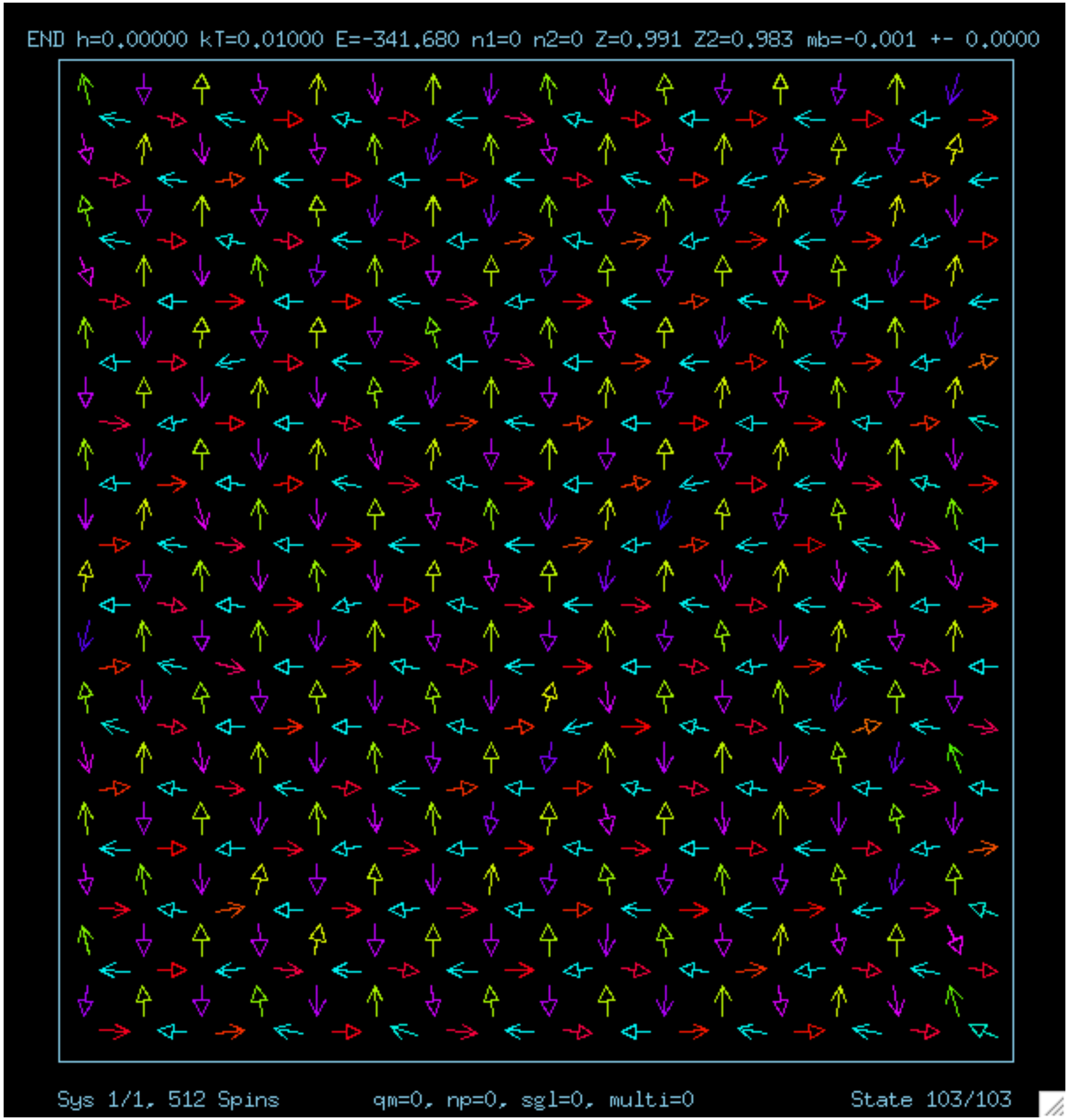

$D = 0.1$

$K_1=0.1$

$K_3=0.5$

$kT=0.01$

$\approx$ ground state

(from long-time Langevin dynamics)

$$D = \frac{\mu_0}{4\pi}\frac{\mu^2}{a^3}$$

artificial ice model

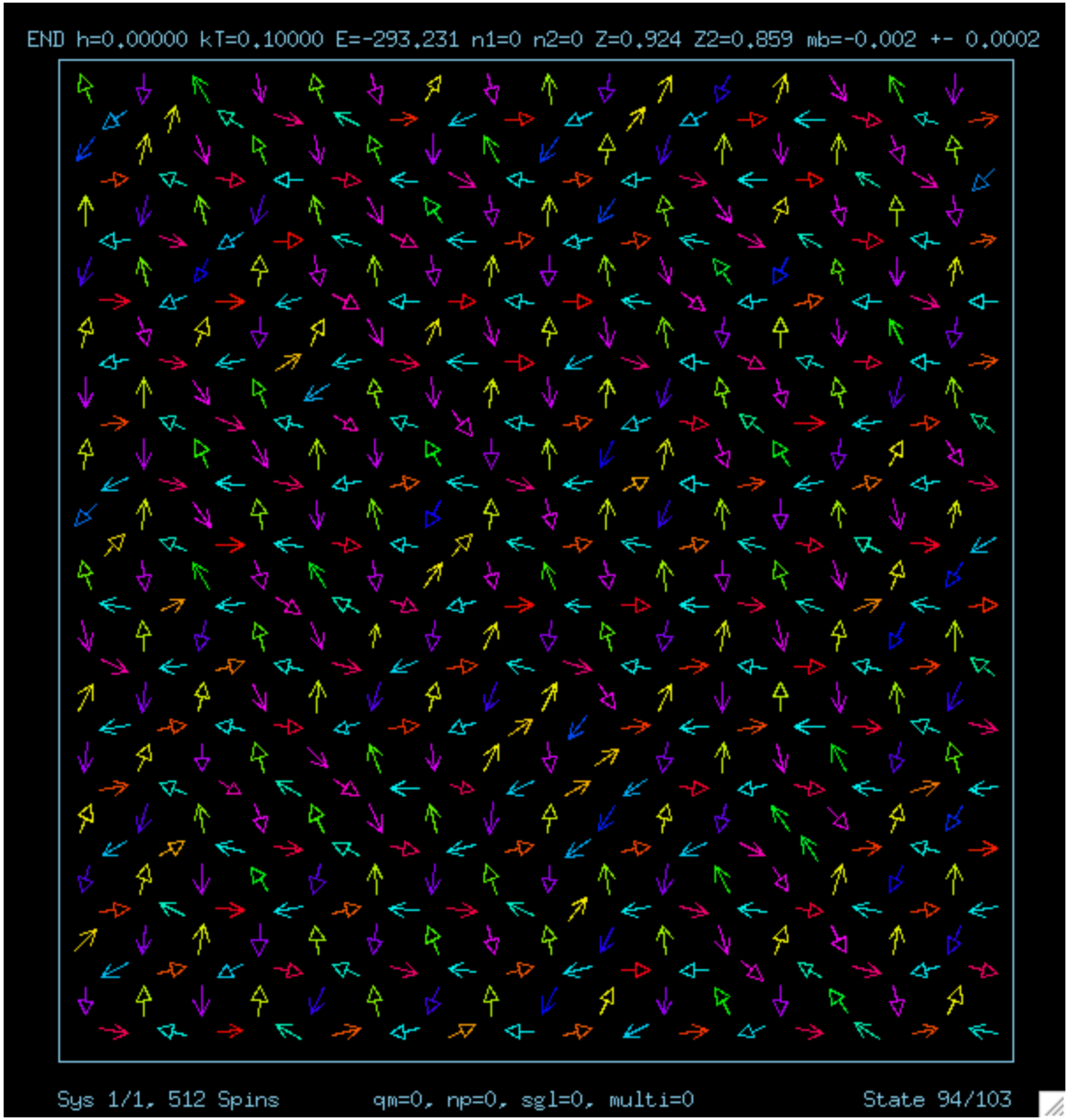

$D = 0.1$
$K_1=0.1$
$K_3=0.5$

$kT=0.10$

> ground state

(from long-time Langevin dynamics)

artificial ice model

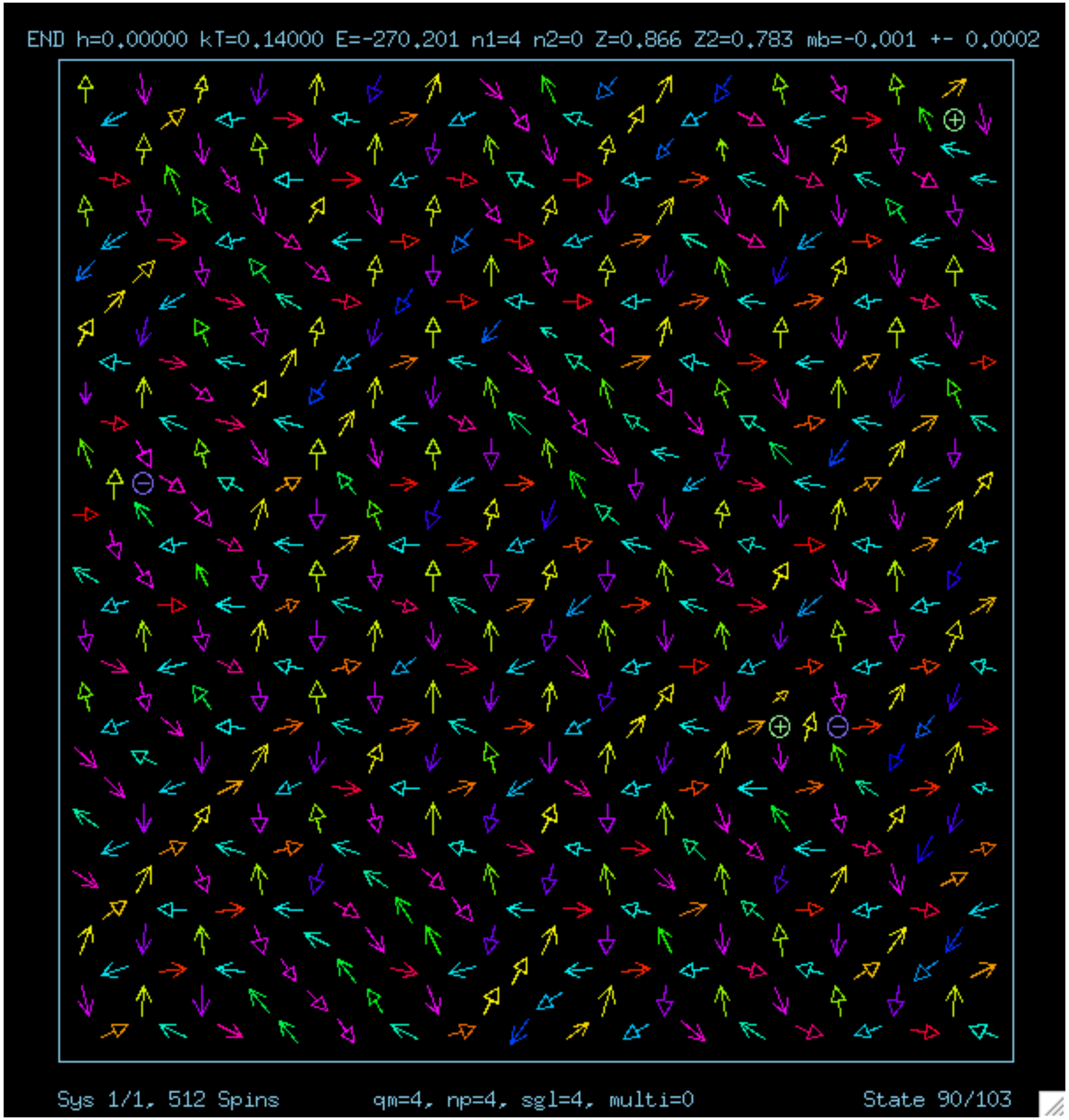

$D = 0.1$

$K_1=0.1$

$K_3=0.5$

$kT=0.14$

few monopoles

(from long-time
Langevin dynamics)

artificial ice model

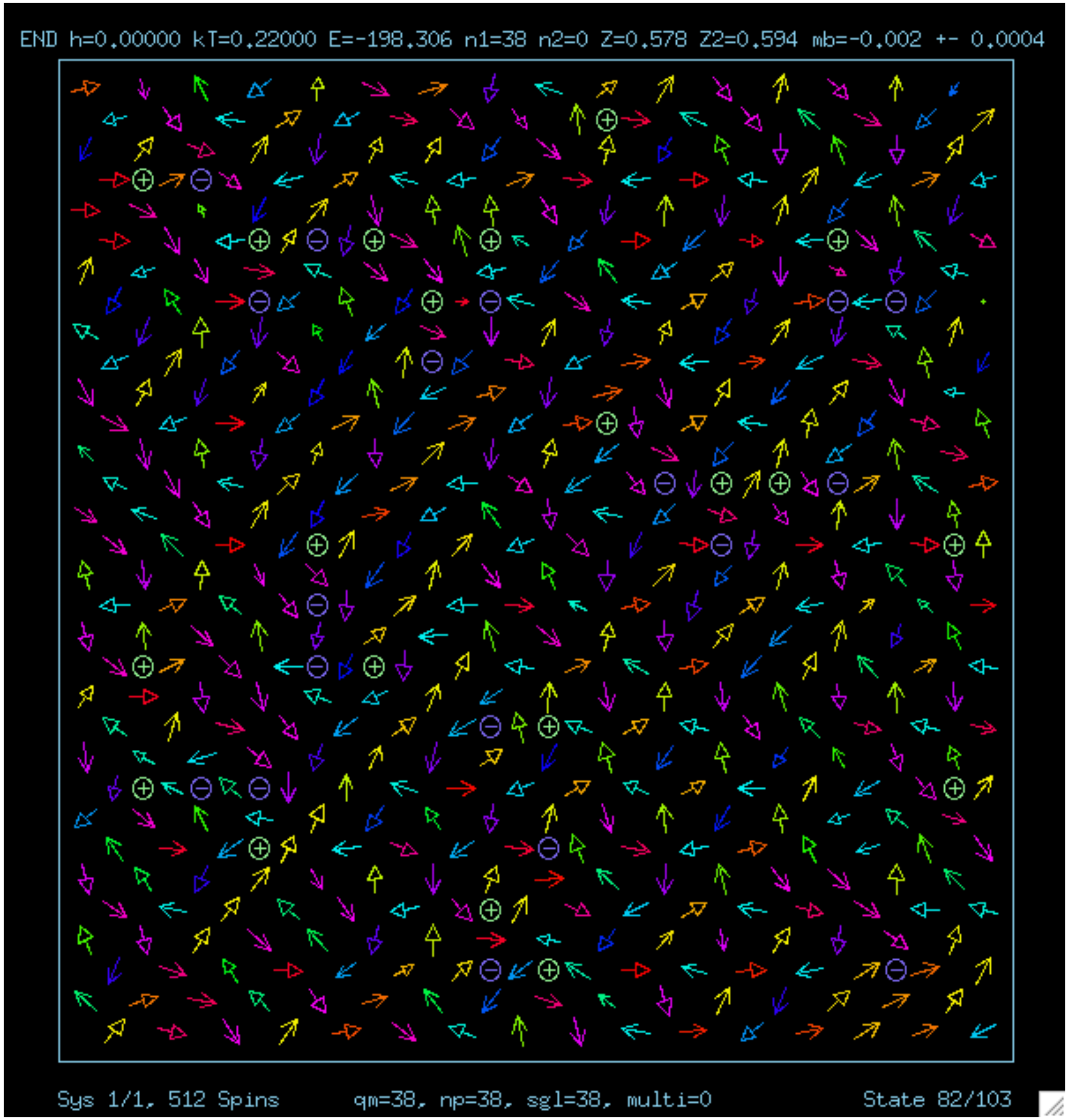

$D = 0.1$
$K_1=0.1$
$K_3=0.5$

$kT=0.22$

$\approx$ transition to high-T phase

(from long-time Langevin dynamics)

artificial ice model

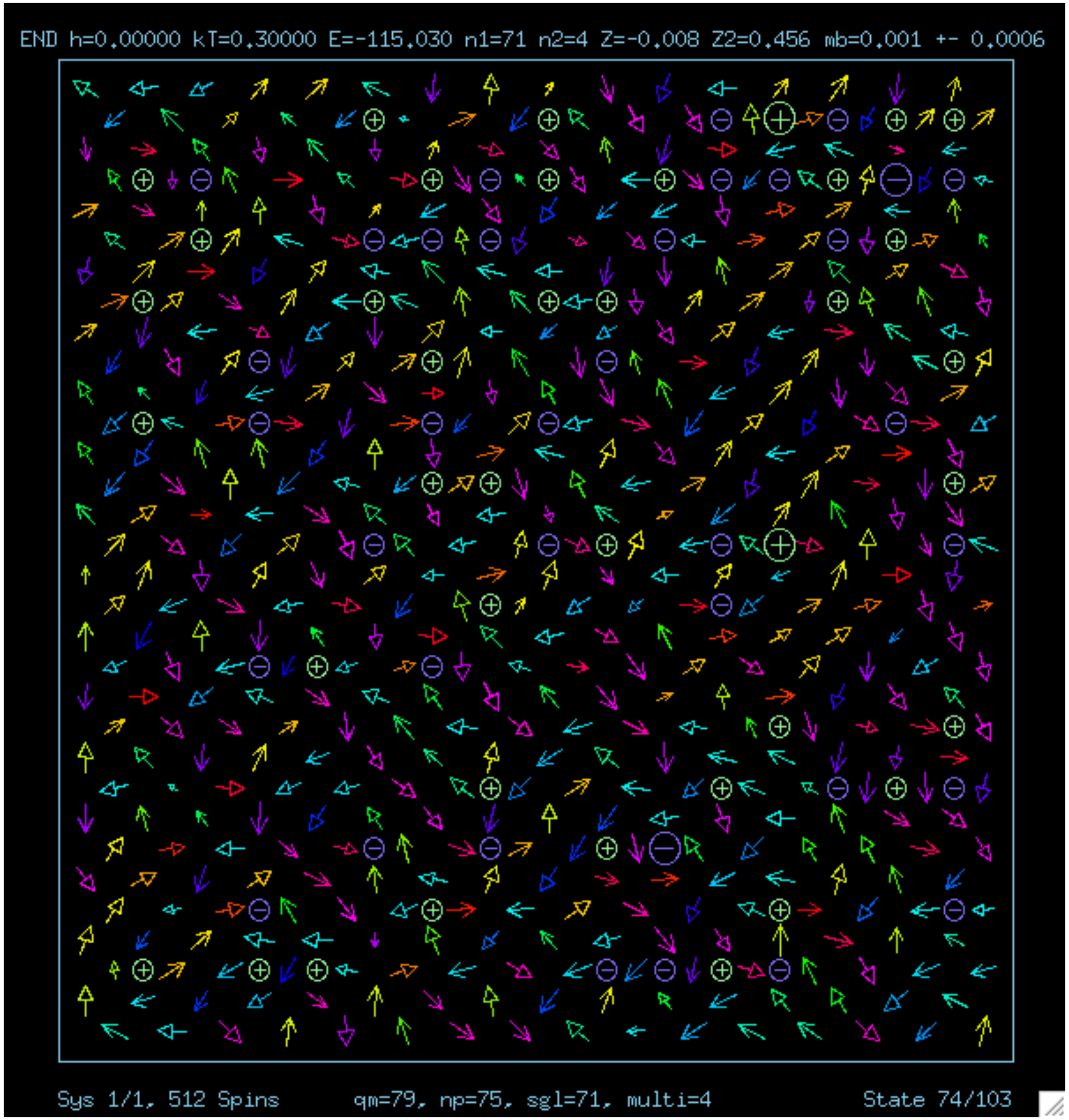

$D = 0.1$

$K_1 = 0.1$

$K_3 = 0.5$

$kT = 0.30$

$\approx$ high-T disorder

(from long-time Langevin dynamics)

Typical thermodynamics shows a phase transition

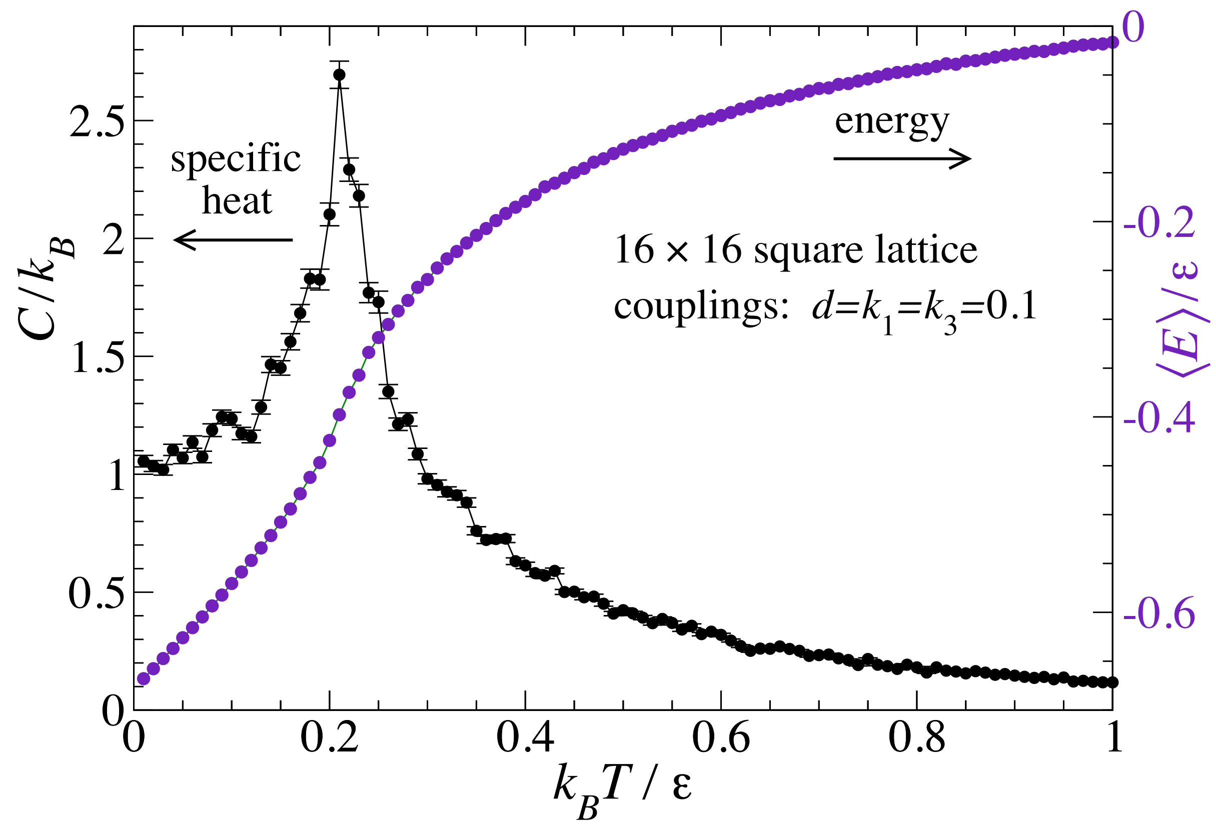

energy and specific heat per island.

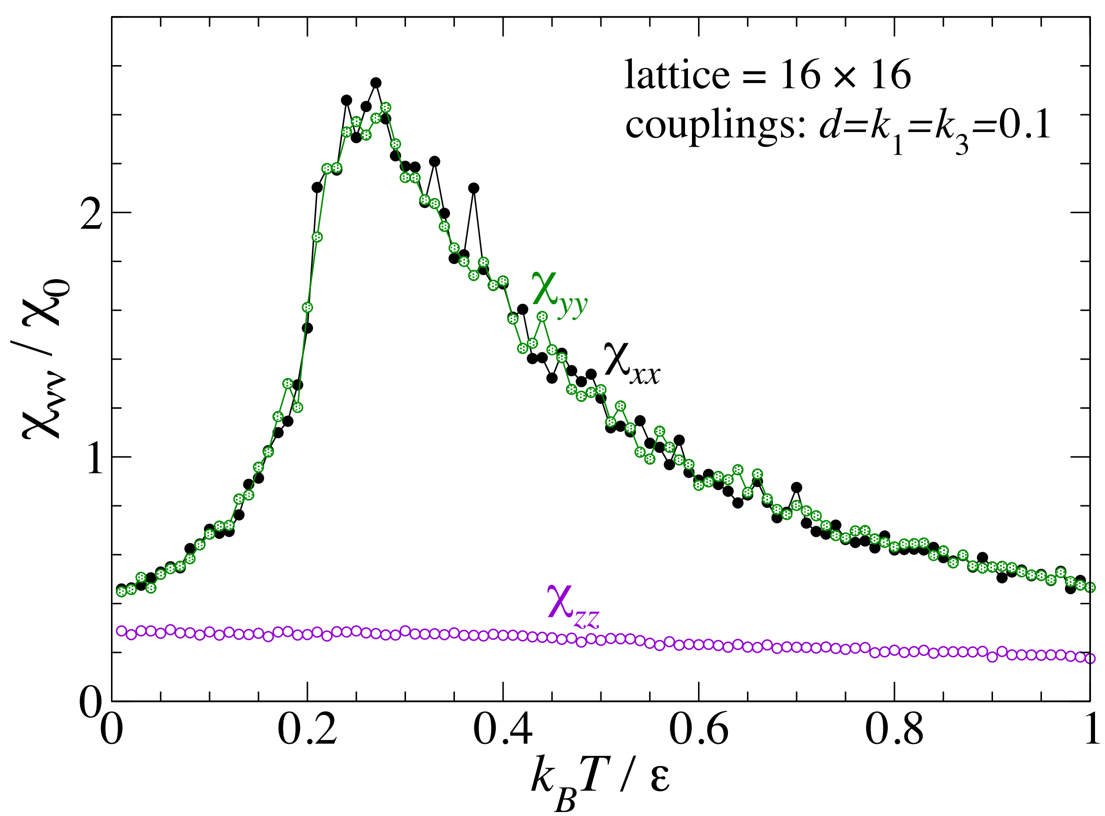

magnetic susceptibilities per island.

Densities of single, double, and total monopoles.

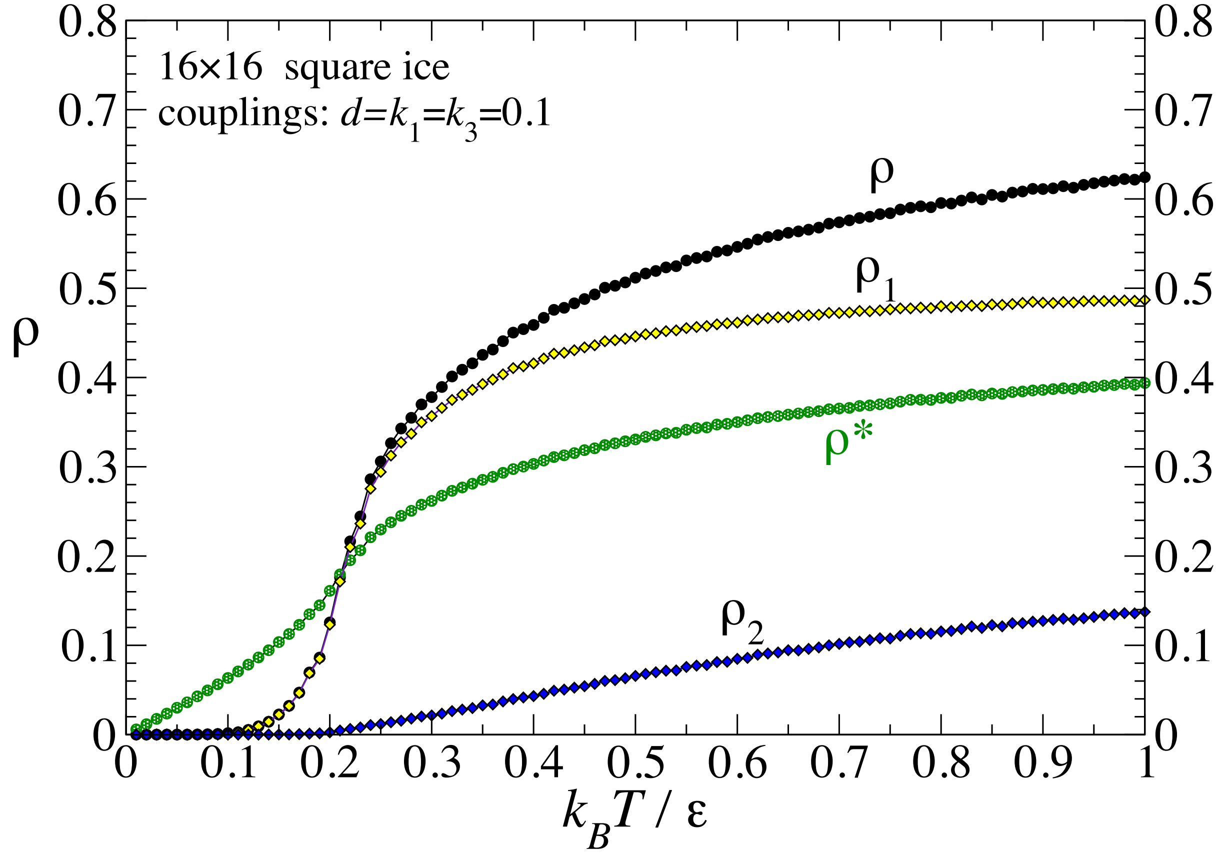

Order parameter Z measures alignment to a ground state.

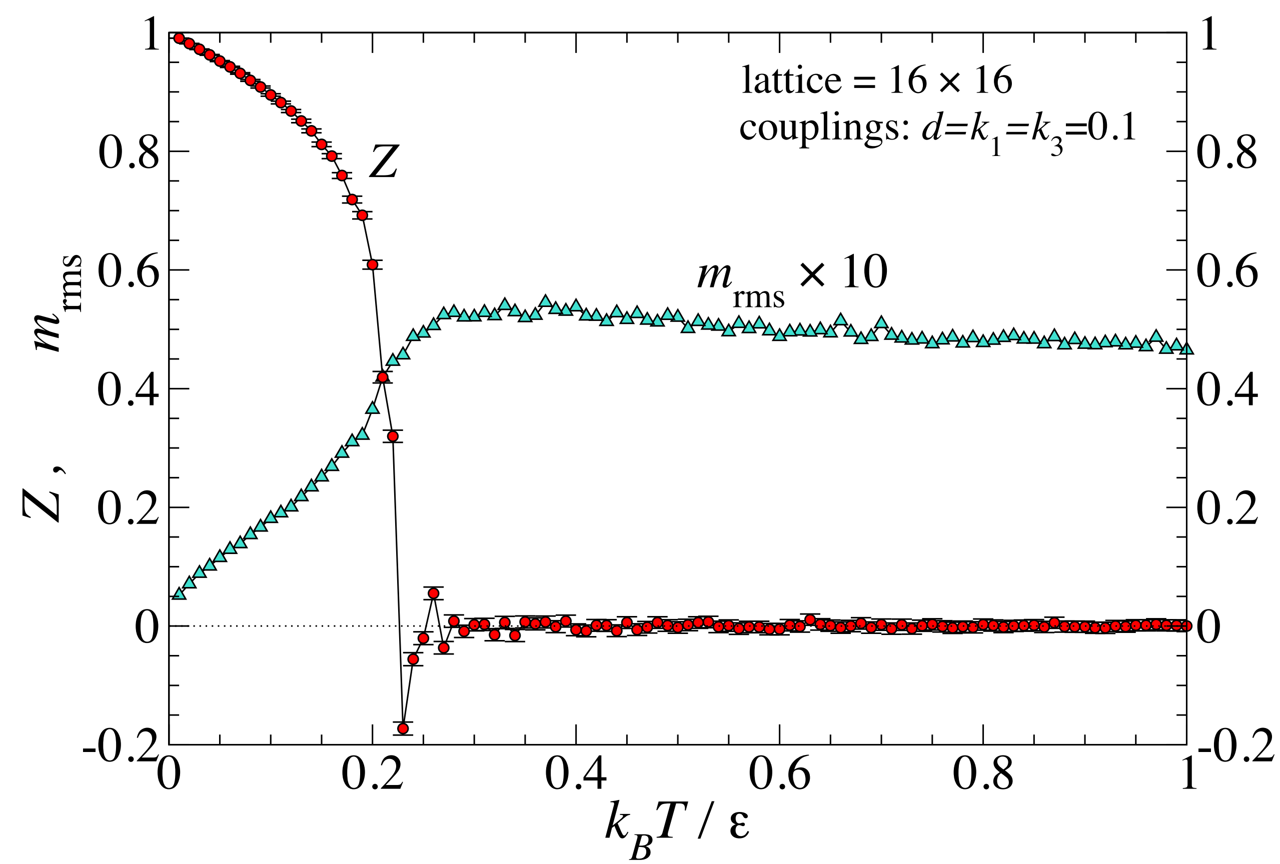

scanning through applied magnetic field.

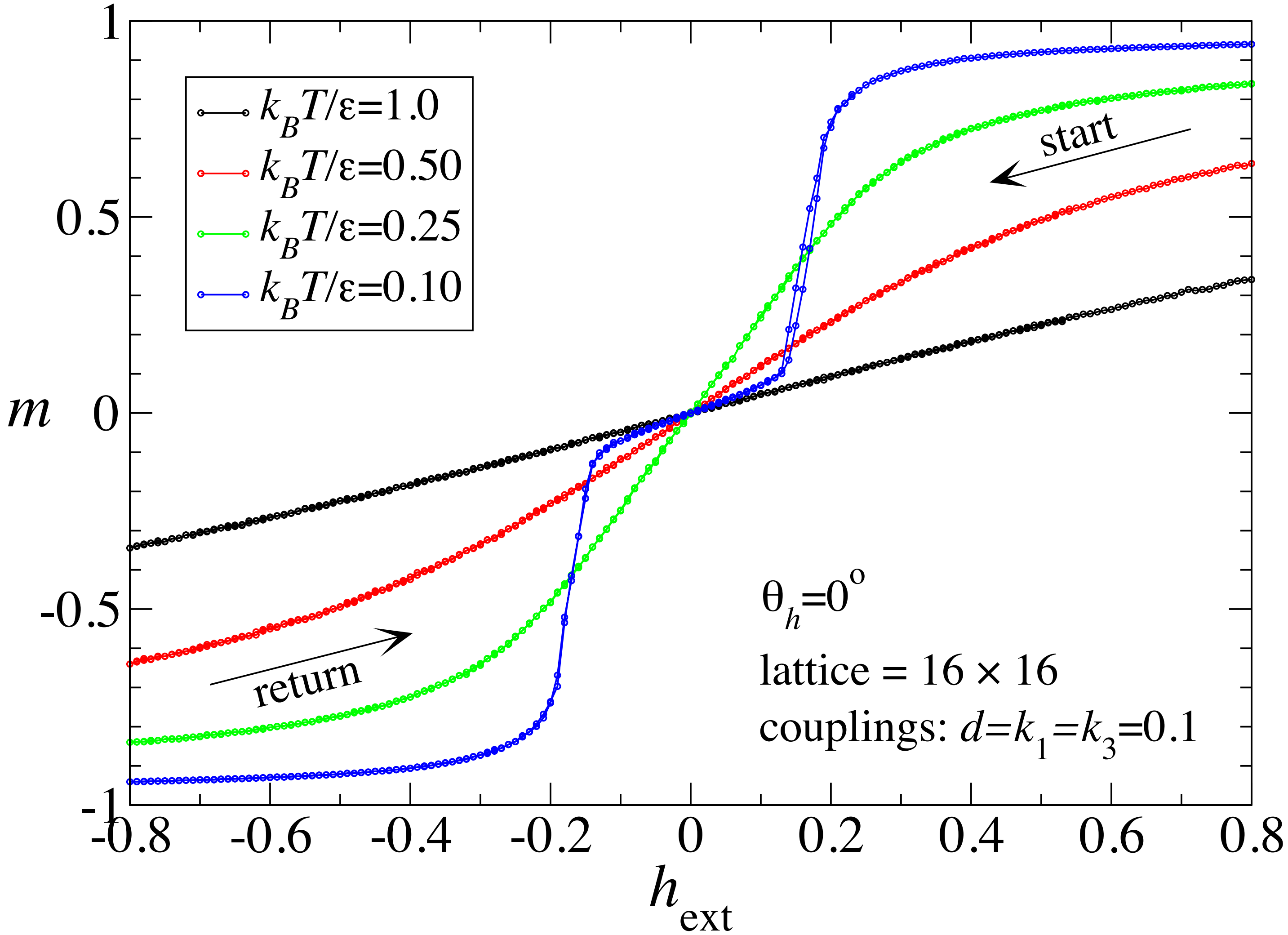

The hysteresis curve deforms when the ground state is approached (low-T, blue curve).

ice model for Wang et al (2006) particles

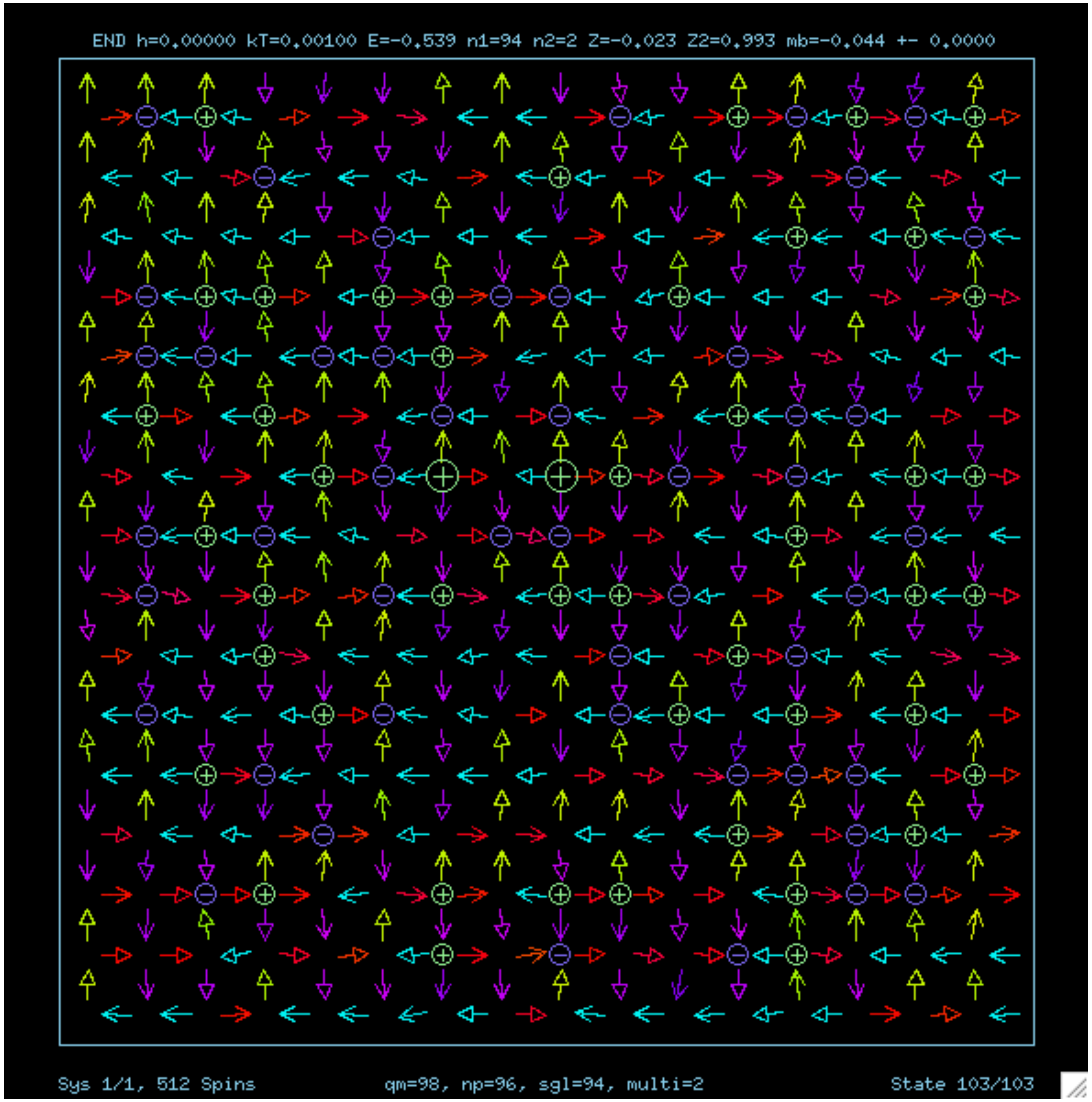

$D = 0.000835$
$K_1=0.0897$
$K_3=0.2000$

$kT=0.001$

$\neq$ ground state

(from long-time Langevin dynamics)

Note: 300 K is $kT = 1.29 \times 10^{-5}$

$$D = \frac{\mu_0}{4\pi} \frac{\mu^2}{a^3}$$

ice model for Wang et al (2006) particles

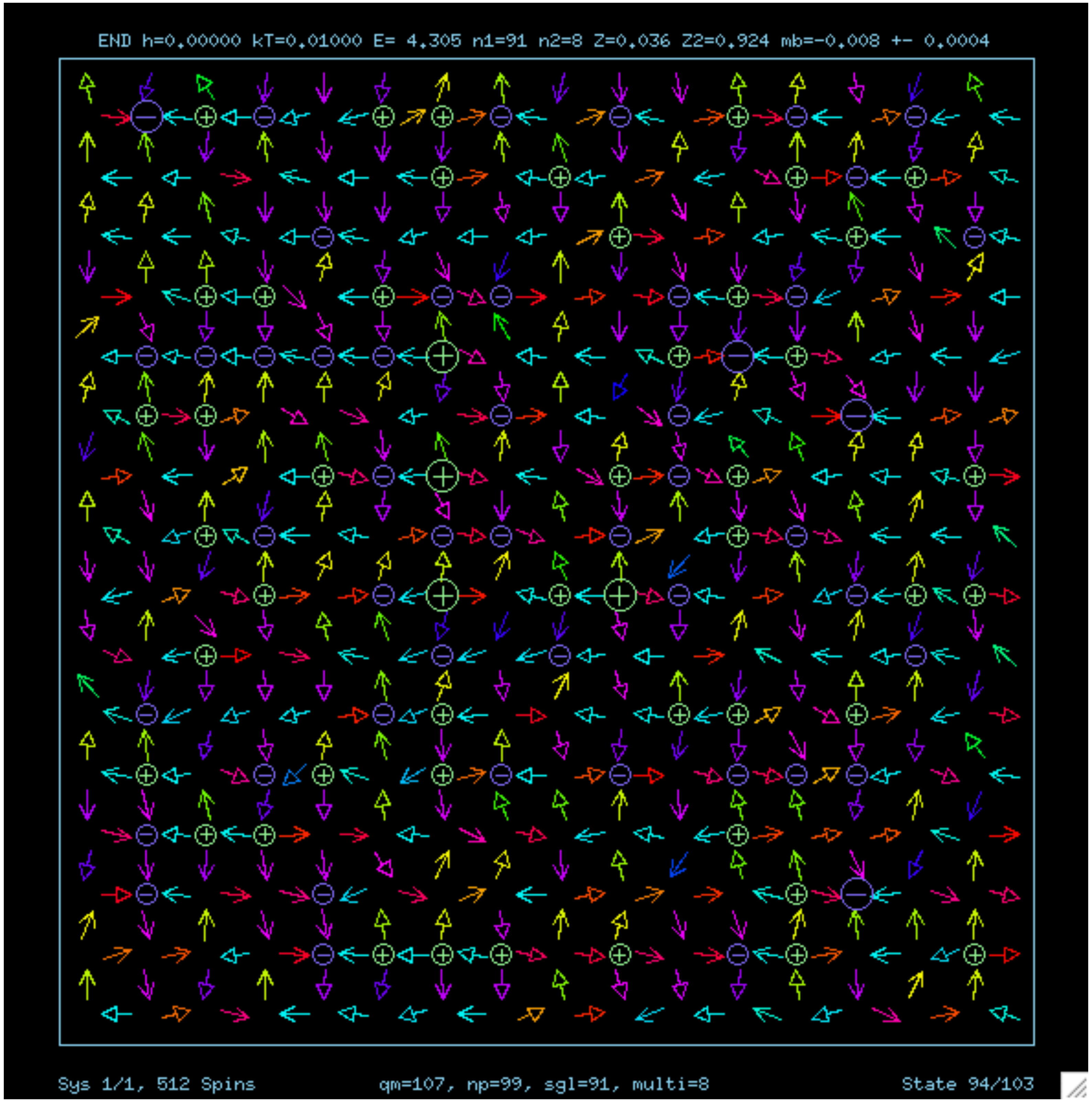

$D = 0.000835$

$K_1 = 0.0897$

$K_3 = 0.2000$

$kT = 0.01$

$\neq$ ground state

(from long-time Langevin dynamics)

ice model for Wang et al (2006) particles

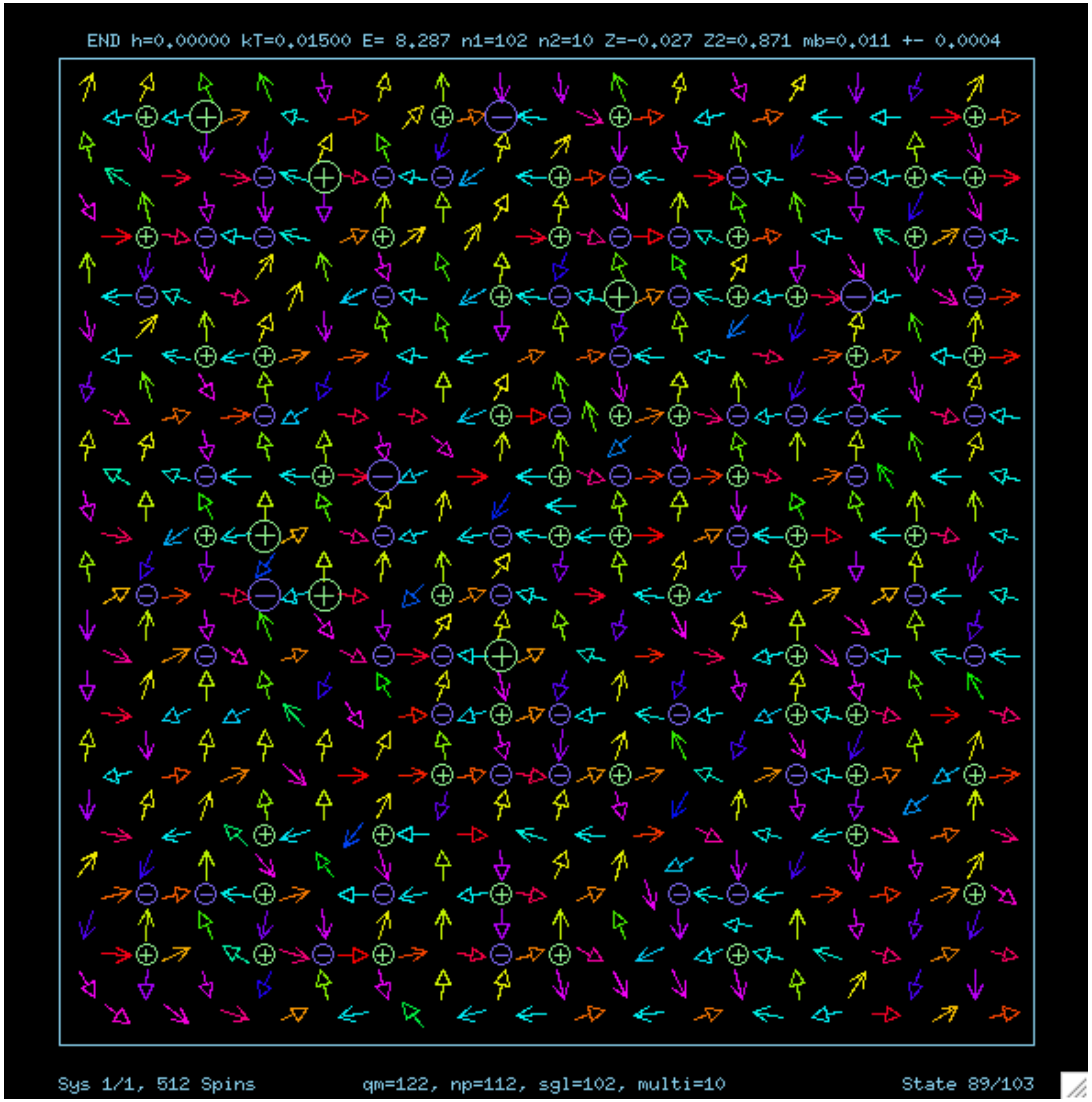

$D = 0.000835$
$K_1 = 0.0897$
$K_3 = 0.2000$

$kT = 0.015$

more monopoles

(from long-time Langevin dynamics)

ice model for Wang et al (2006) particles

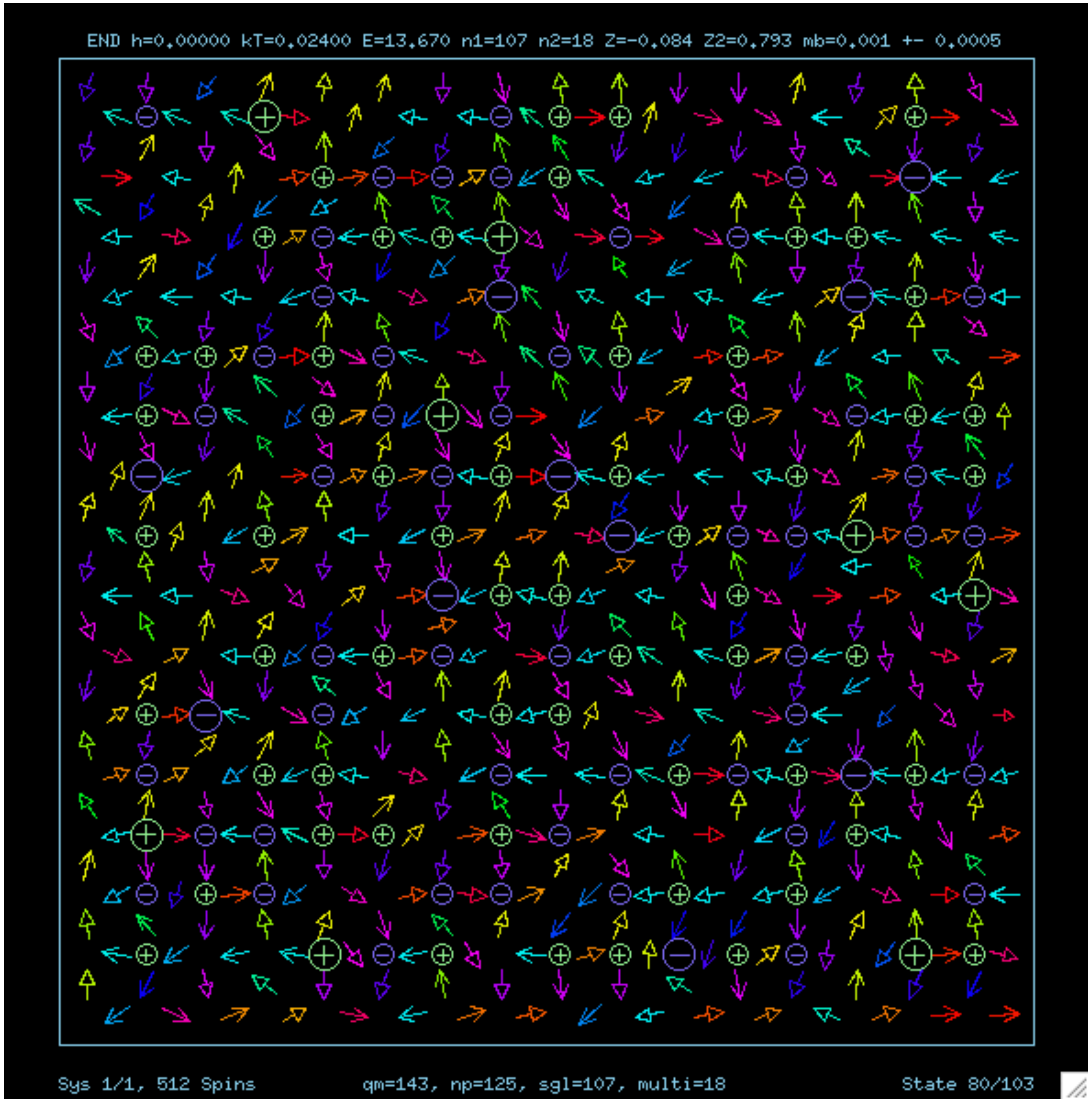

$D = 0.000835$

$K_1=0.0897$

$K_3=0.2000$

$kT=0.024$

more monopoles

(from long-time
Langevin dynamics)

ice model for Wang et al (2006) particles

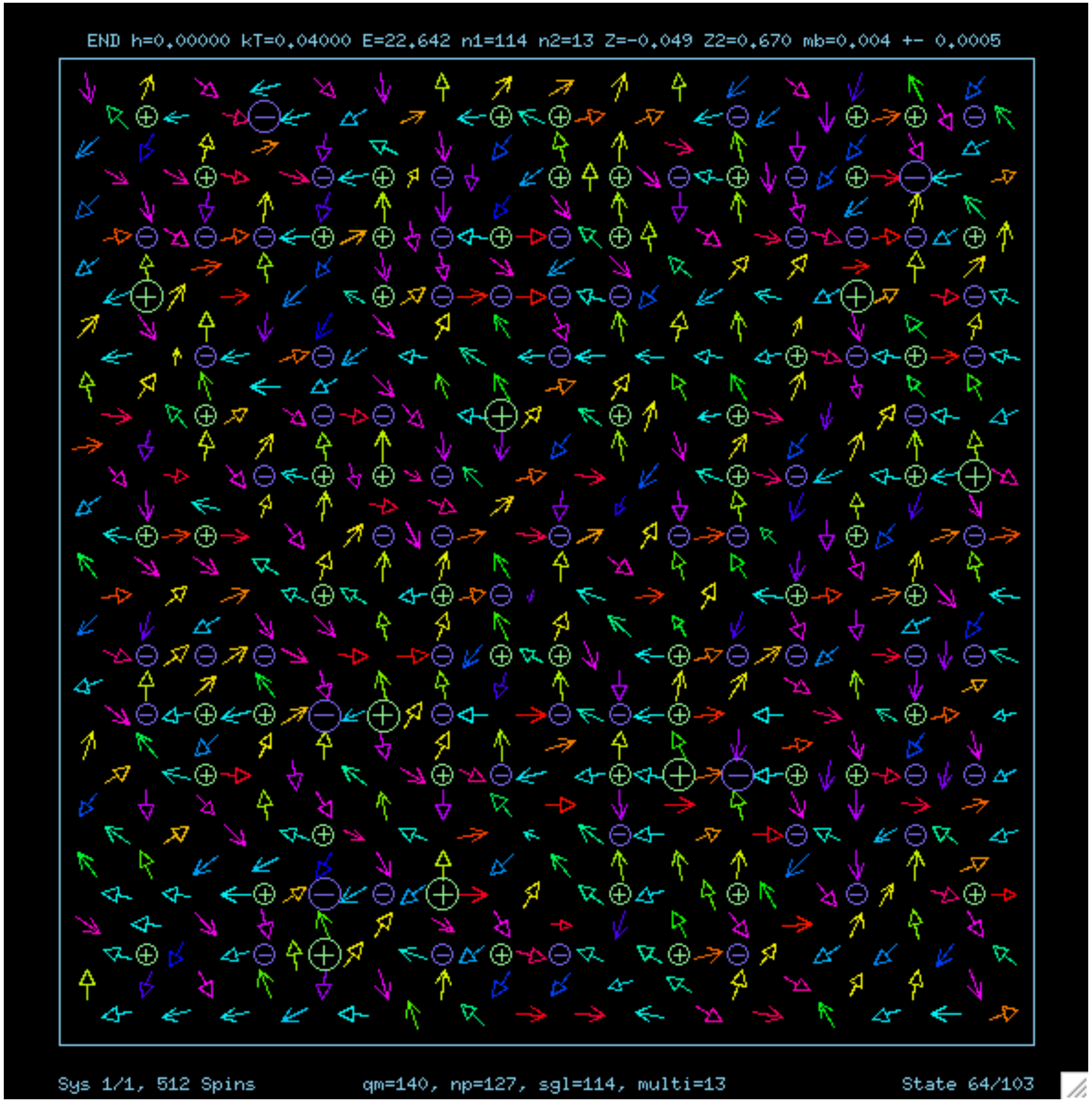

$D = 0.000835$

$K_1 = 0.0897$

$K_3 = 0.2000$

$kT = 0.040$

highly disordered

(from long-time Langevin dynamics)

artificial ice model - Kagomé lattice

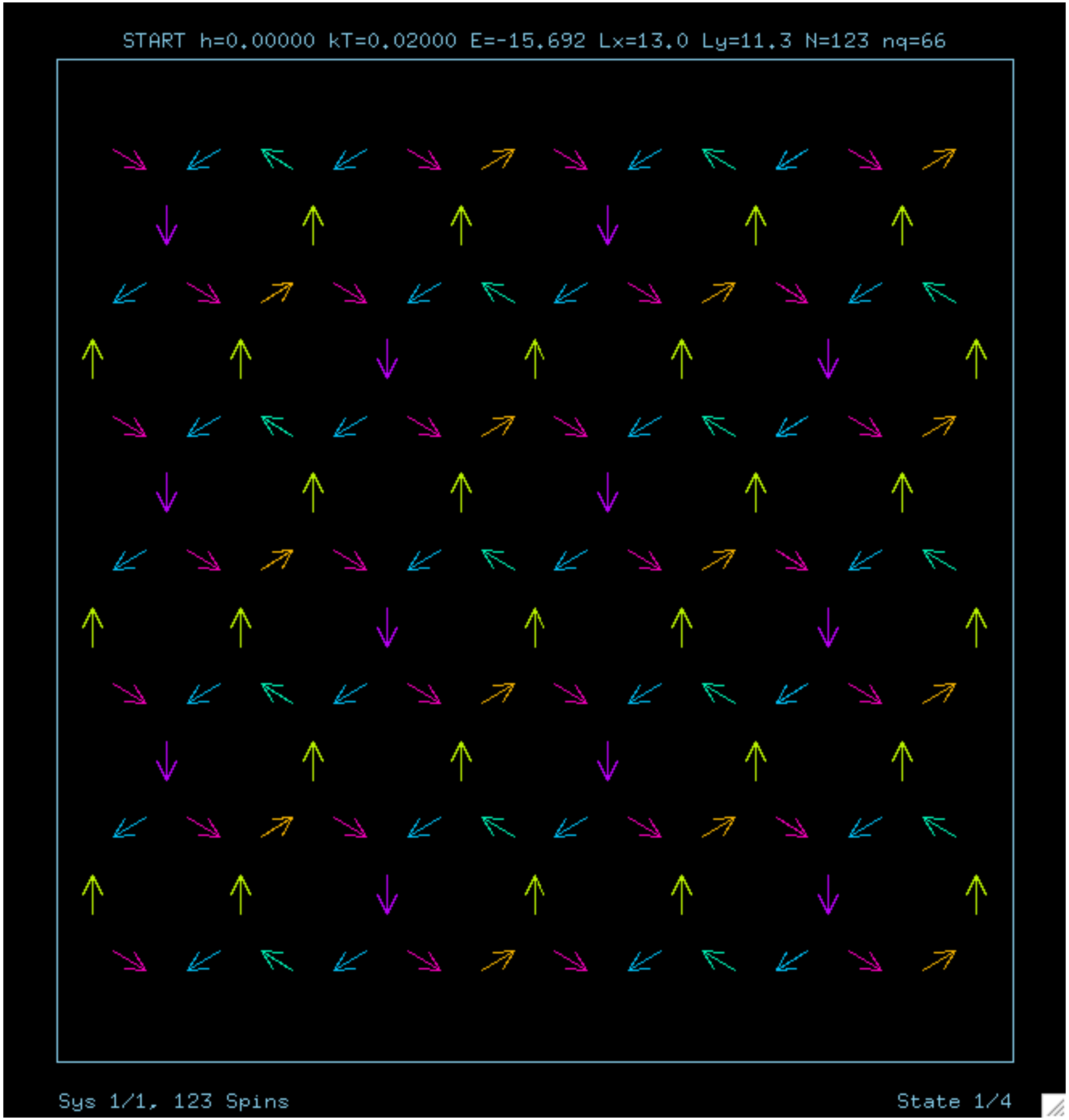

$D = 0.1$
$K_1 = 0.1$
$K_3 = 0.5$

1 of 6 ground states

artificial ice model - Kagomé lattice

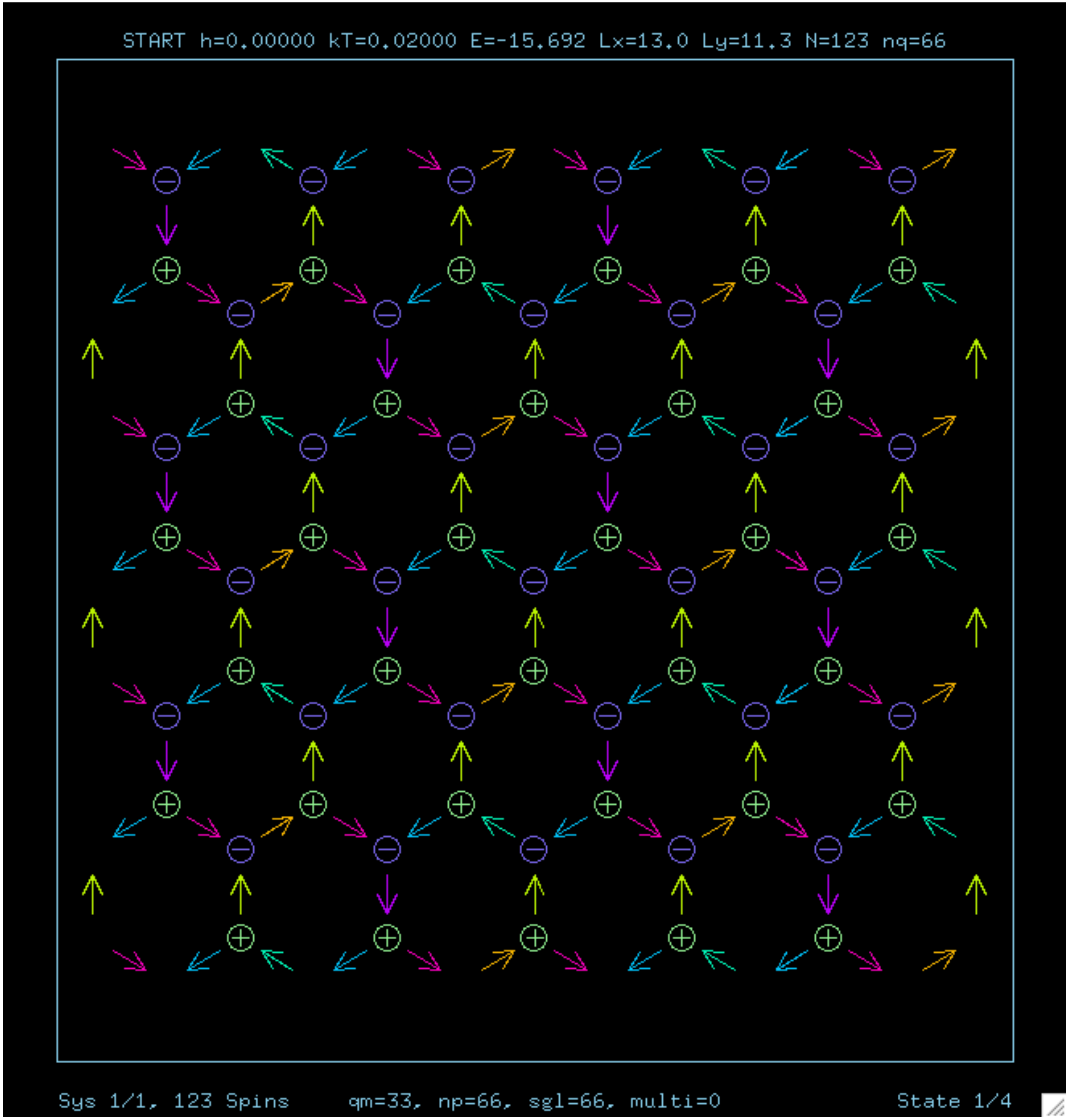

$D = 0.1$

$K_1=0.1$

$K_3=0.5$

1 of 6 ground states

all vertices have a monopole charge.

artificial ice model - Kagomé lattice

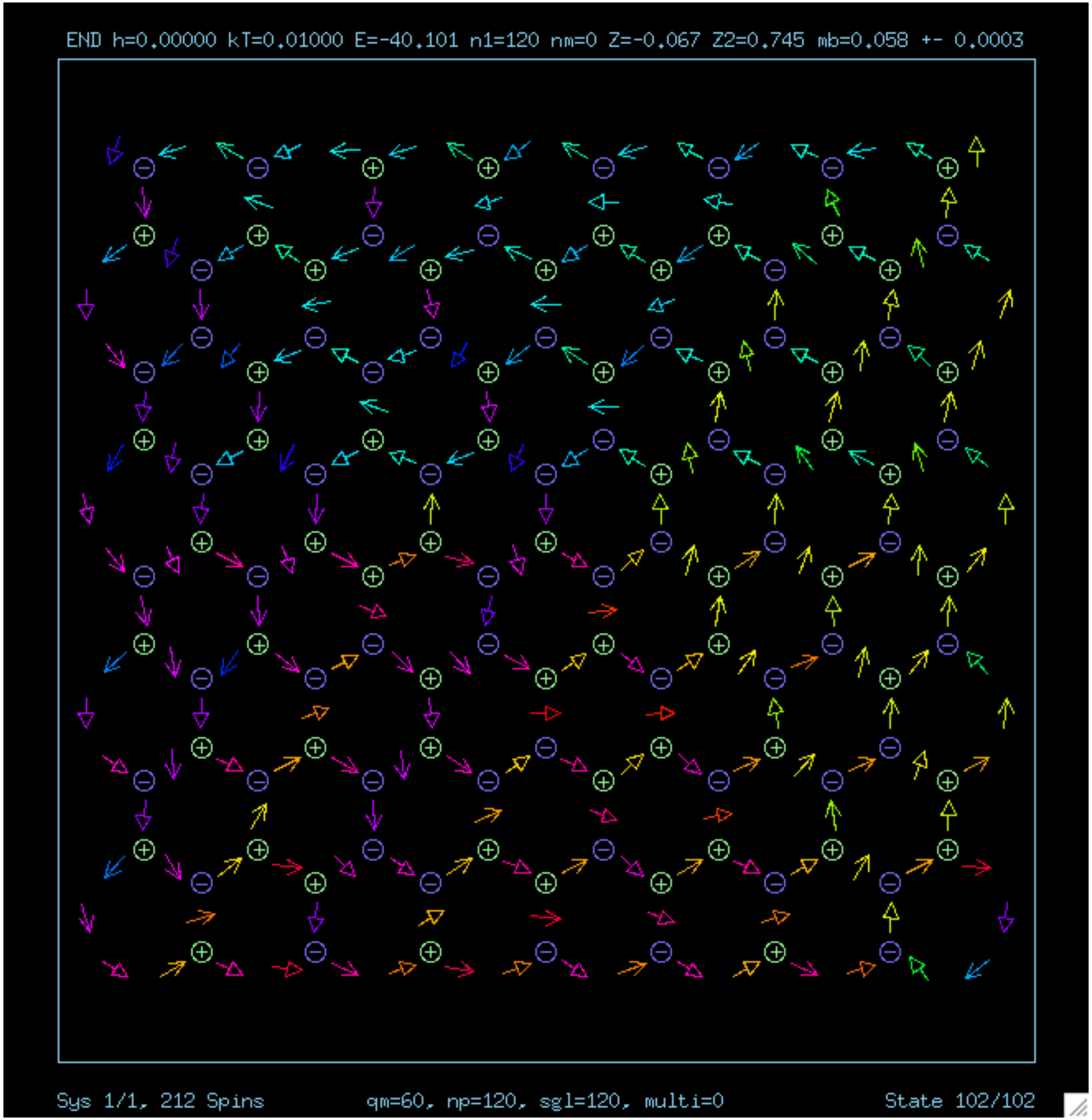

$D = 0.1$

$K_1=0.1$

$K_3=0.5$

kT=0.01 (low T).

Frustrated state does not approach ground state.

(from long-time Langevin dynamics)

artificial ice model - Kagomé lattice

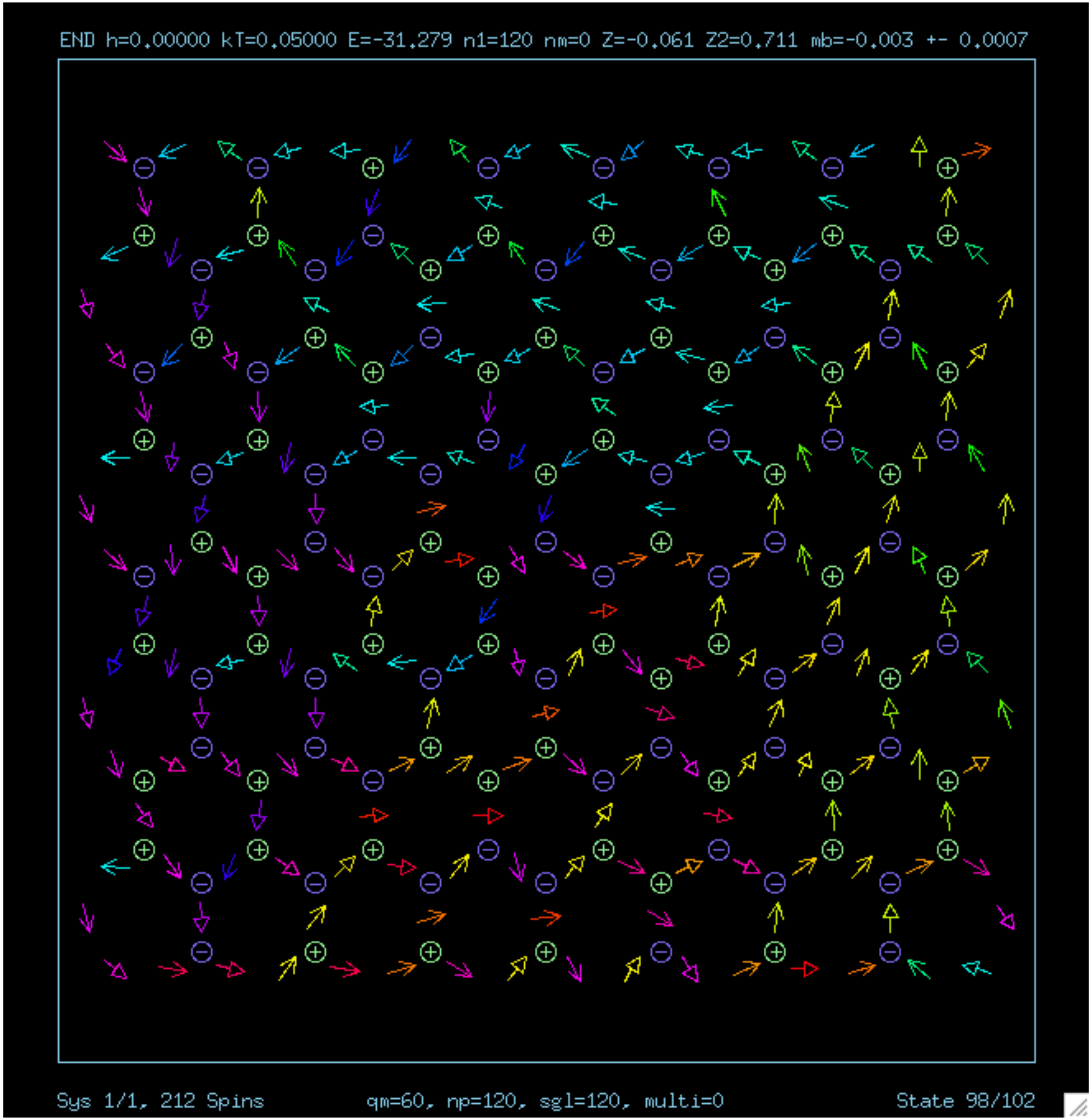

$D = 0.1$
$K_1=0.1$
$K_3=0.5$

$kT=0.05$

(from long-time Langevin dynamics)

artificial ice model - Kagomé lattice

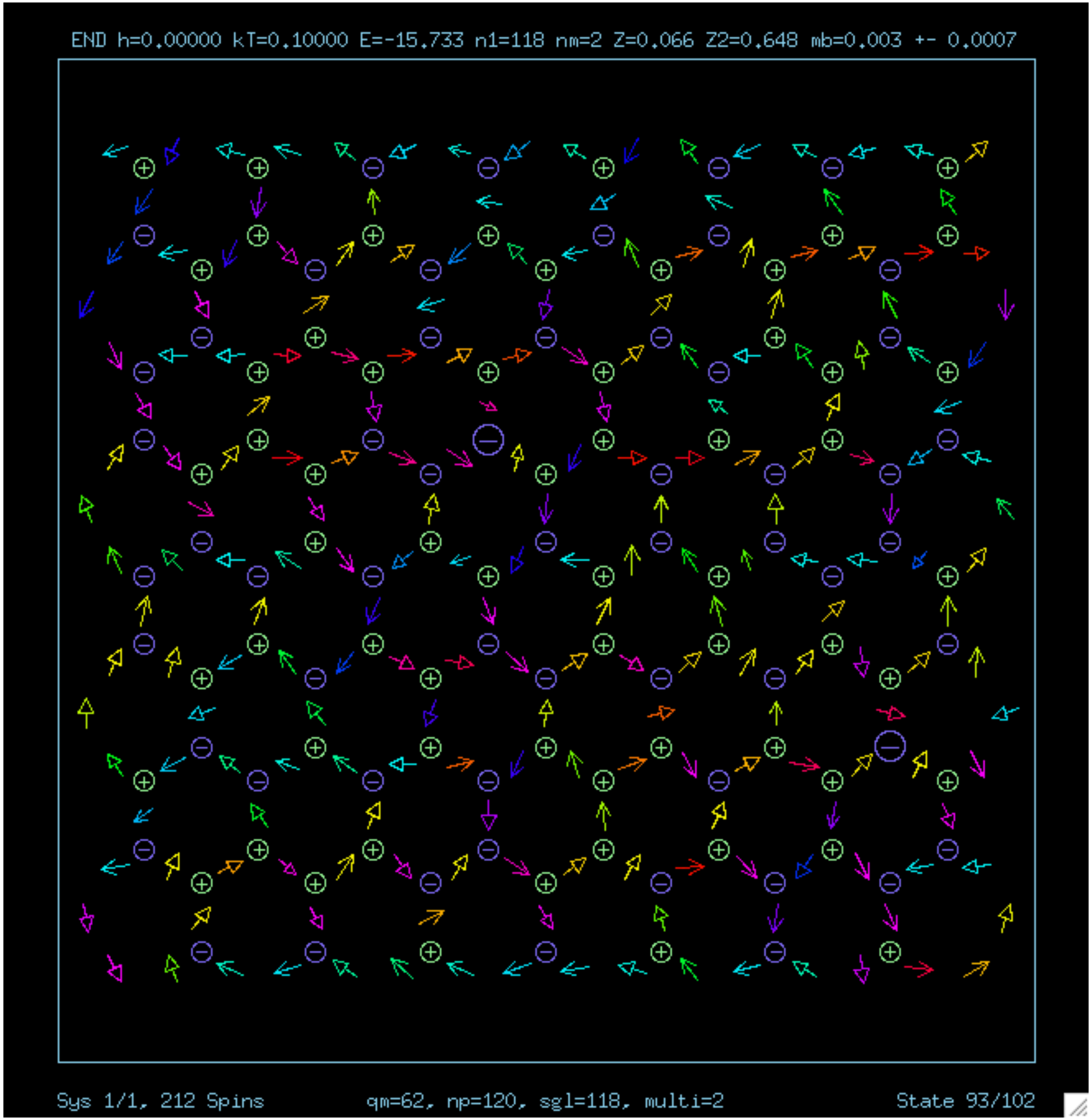

$D = 0.1$

$K_1=0.1$

$K_3=0.5$

$kT=0.1$ (moderate)

multi-charge poles

(from long-time
Langevin dynamics)

artificial ice model - Kagomé lattice

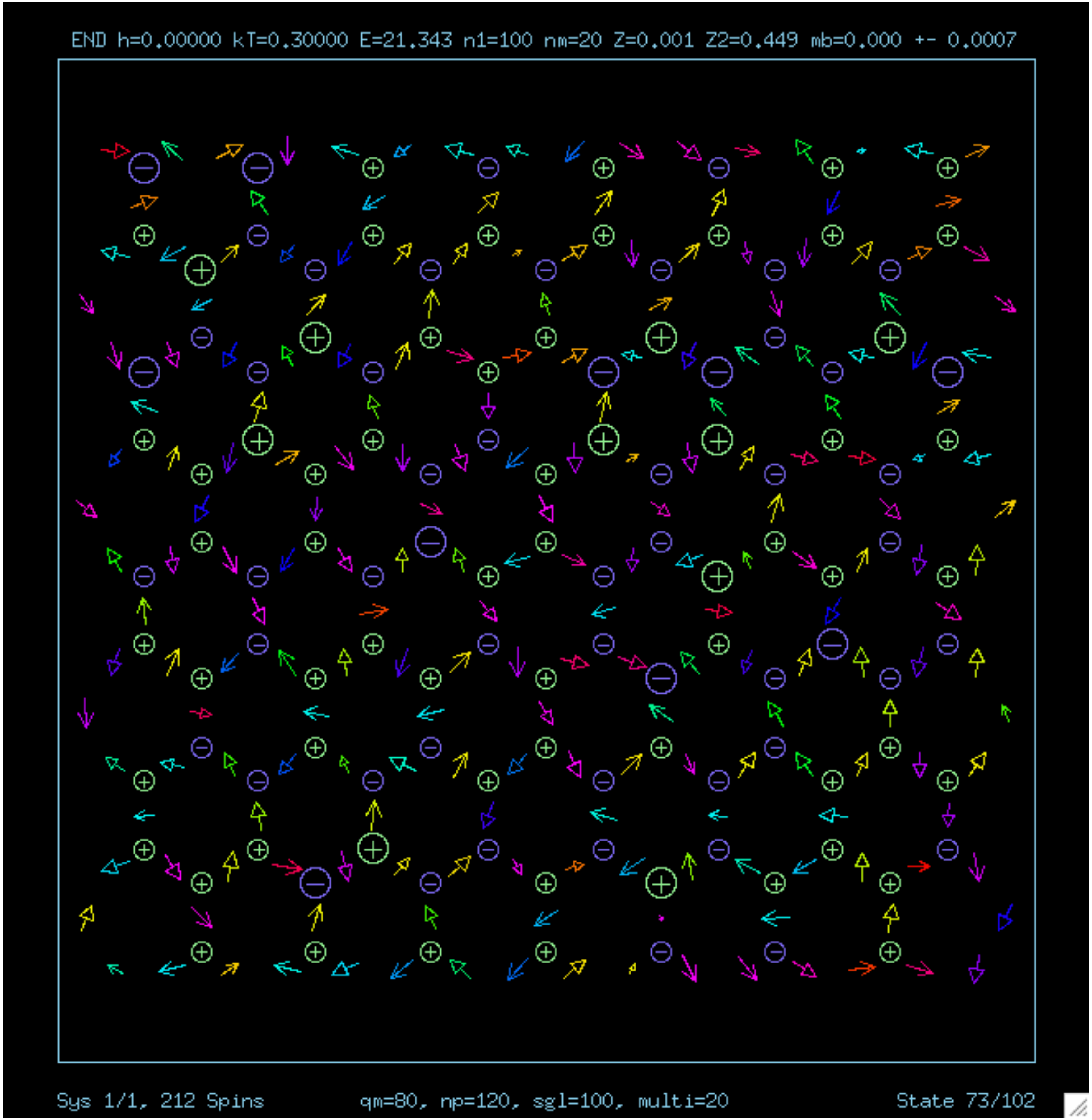

$D = 0.1$

$K_1=0.1$

$K_3=0.5$

kT=0.3 (high)

many
multi-charge poles

(from long-time
Langevin dynamics)

What about linearized (small amplitude) oscillations at low temperature? (work by Thomas Lasnier)

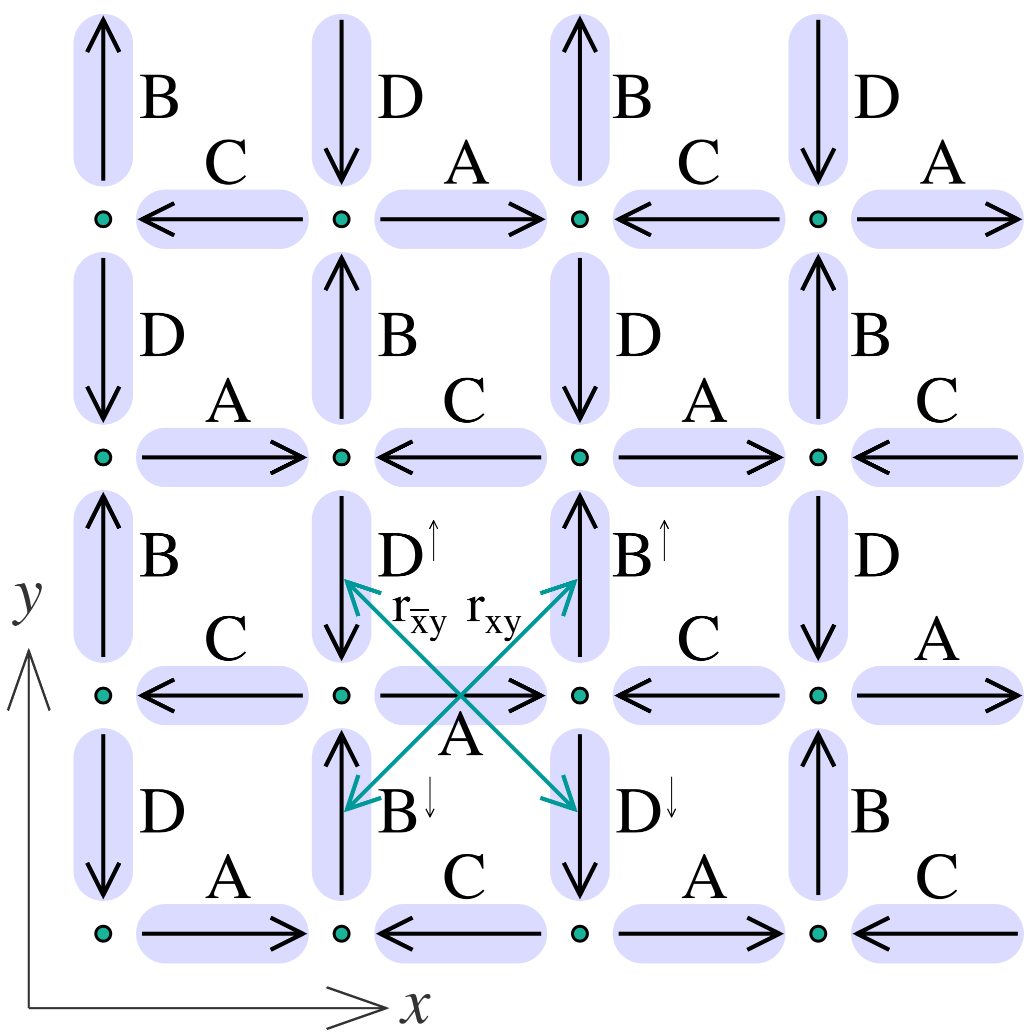

A square ice ground state.
Notation for deviations around a site A.
Keep only near neighbor interactions.
There are four sublattices!

Hamiltonian:

$$\mathcal{H} = -\frac{\mu_0}{4\pi}\frac{\mu^2}{a^3}\sum_{i>j}\frac{[3(\hat{\boldsymbol{\mu}}_i\cdot\hat{\mathbf{r}}_{ij})(\hat{\boldsymbol{\mu}}_j\cdot\hat{\mathbf{r}}_{ij})-\hat{\boldsymbol{\mu}}_i\cdot\hat{\boldsymbol{\mu}}_j]}{(r_{ij}/a)^3} + \sum_i\left\{K_1[1-(\hat{\boldsymbol{\mu}}_i\cdot\hat{\mathbf{u}}_i)^2]+K_3(\hat{\boldsymbol{\mu}}_i\cdot\hat{\mathbf{z}})^2\right\}$$

effective field:

$$\mathbf{B}_i = -\frac{\delta\mathcal{H}}{\delta\boldsymbol{\mu}_i}$$

Eq. of motion:

$$\frac{d\hat{\boldsymbol{\mu}}_i}{dt} = \gamma_{\mathrm{e}}\hat{\boldsymbol{\mu}}_i\times\mathbf{B}_i.$$

$$\hat{\boldsymbol{\mu}}_i \equiv \mathbf{A}$$

$$\boxed{\frac{d\mathbf{A}}{dt} = \mathbf{A}\times\mathbf{F}(\mathrm{A})}$$

$$\begin{aligned}\mathbf{F}(\mathrm{A}) = {} & \kappa_1 A_x\hat{\mathbf{x}} - \kappa_3 A_z\hat{\mathbf{z}} \\ & +\delta_1\Big\{3\left[(\mathbf{B}^{\uparrow}+\mathbf{B}^{\downarrow})\cdot\hat{\mathbf{r}}_{\mathrm{xy}}\right]\hat{\mathbf{r}}_{\mathrm{xy}} - \mathbf{B}^{\uparrow} - \mathbf{B}^{\downarrow} \\ & \quad +3\left[(\mathbf{D}^{\uparrow}+\mathbf{D}^{\downarrow})\cdot\hat{\mathbf{r}}_{\bar{\mathrm{x}}\mathrm{y}}\right]\hat{\mathbf{r}}_{\bar{\mathrm{x}}\mathrm{y}} - \mathbf{D}^{\uparrow} - \mathbf{D}^{\downarrow}\Big\}\end{aligned}$$

Also get eqns. for dB/dt, dC/dt, dD/dt .

Linearization: Assume small deviations:

$$
\begin{aligned}
\mathbf{A} &= \mathbf{A}_0 + \mathbf{a} = (1 + a_x, a_y, a_z),\\
\mathbf{B} &= \mathbf{B}_0 + \mathbf{b} = (b_x, 1 + b_y, b_z),\\
\mathbf{C} &= \mathbf{C}_0 + \mathbf{c} = (-1 + c_x, c_y, c_z),\\
\mathbf{D} &= \mathbf{D}_0 + \mathbf{d} = (d_x, -1 + d_y, d_z).
\end{aligned}
$$

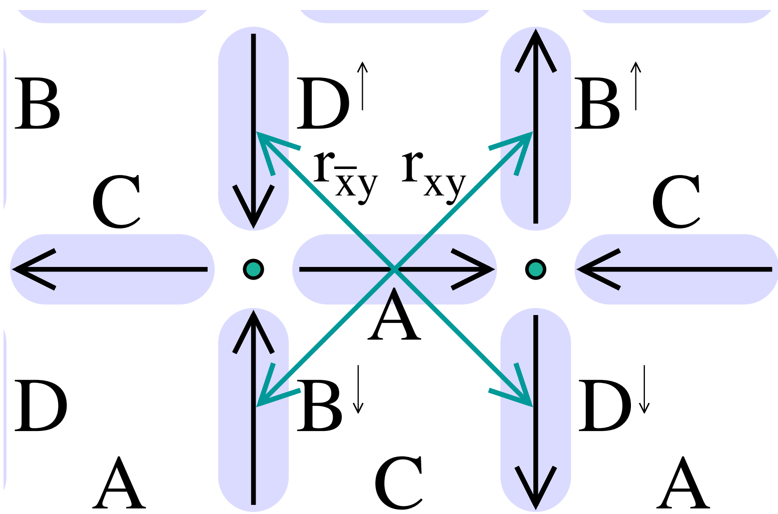

You get a simple 8x8 eigenvalue problem.

$$
\begin{aligned}
-\mathrm{i}\omega a_y &= \delta_1(6a_z + ub_z + vd_z) + \kappa_{13}a_z,\\
-\mathrm{i}\omega a_z &= \delta_1(-6a_y + \tfrac{3}{2}ub_x - \tfrac{3}{2}vd_x) - \kappa_1 a_y,\\
-\mathrm{i}\omega b_x &= \delta_1(-6b_z - ua_z - vc_z) - \kappa_{13}b_z,\\
-\mathrm{i}\omega b_z &= \delta_1(6b_x - \tfrac{3}{2}ua_y + \tfrac{3}{2}vc_y) + \kappa_1 b_x,\\
-\mathrm{i}\omega c_y &= \delta_1(-6c_z - ud_z - vb_z) + \kappa_{13}c_z,\\
-\mathrm{i}\omega c_z &= \delta_1(6c_y - \tfrac{3}{2}ud_x + \tfrac{3}{2}vb_x) - \kappa_1 c_y,\\
-\mathrm{i}\omega d_x &= \delta_1(6d_z + uc_z + va_z) - \kappa_{13}d_z,\\
-\mathrm{i}\omega d_z &= \delta_1(-6d_x + \tfrac{3}{2}uc_y - \tfrac{3}{2}va_y) + \kappa_1 d_x.
\end{aligned}
$$

and traveling waves:

$$b_x(\mathbf{r}, t) = b_x \mathrm{e}^{\mathrm{i}(\mathbf{q}\cdot\mathbf{r} - \omega t)},$$

wave vector

frequency

Dipole interaction

v = $2\cos[\frac{a}{2}(q_x - q_y)]$

u = $2\cos[\frac{a}{2}(q_x + q_y)]$,

Anisotropy

There are 4 kinds of modes.

2 are <u>antisymmetric</u> across the vertex:

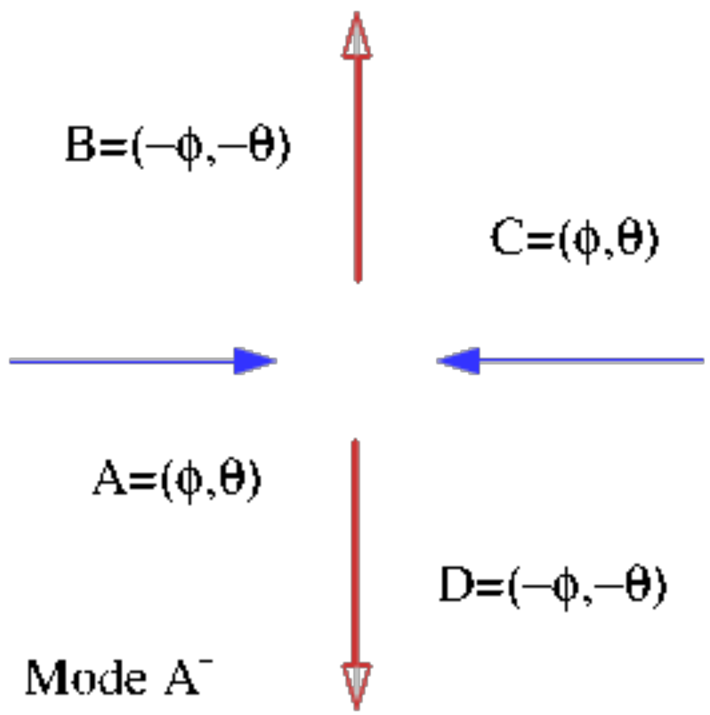

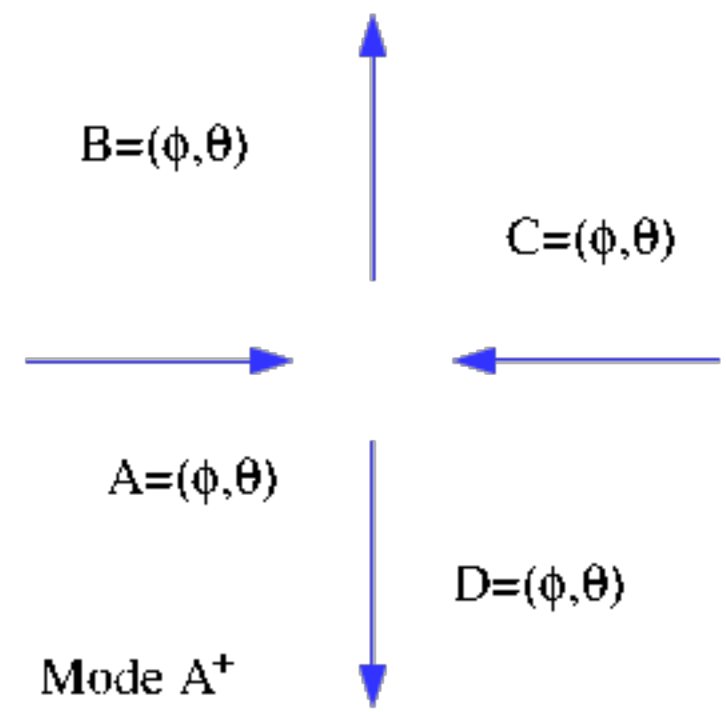

Mode A- has the lowest frequency at long wavelength.

Mode A+ has the highest frequency at long wavelength.

There are 4 kinds of modes.

2 are <u>antisymmetric</u> across the vertex:

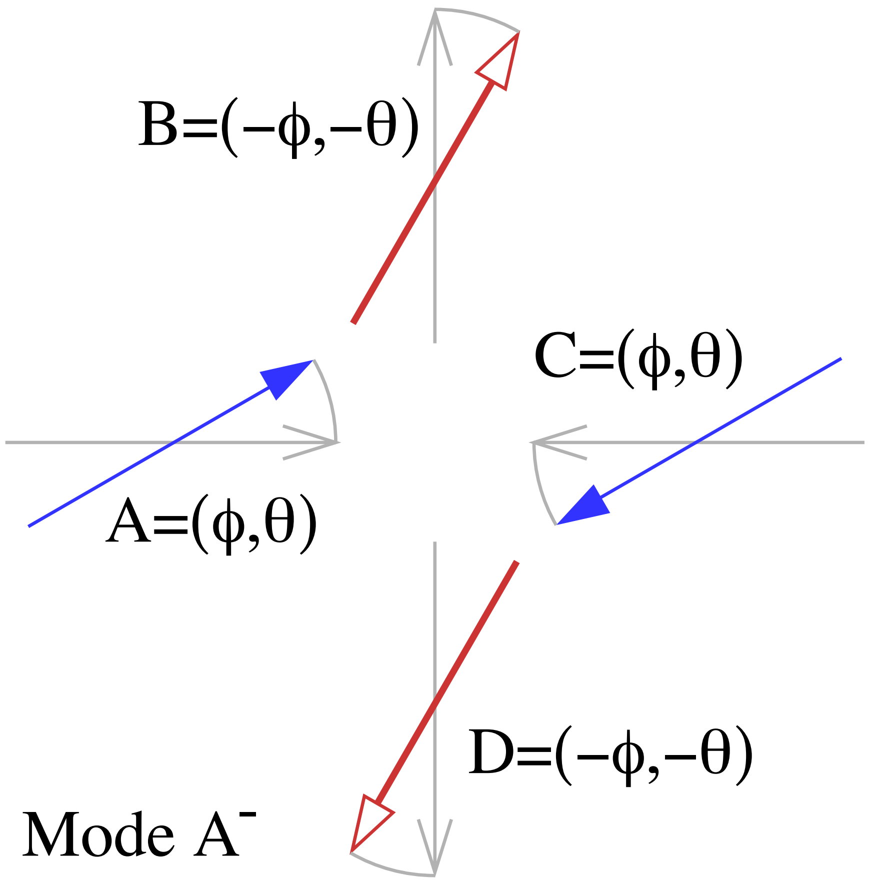

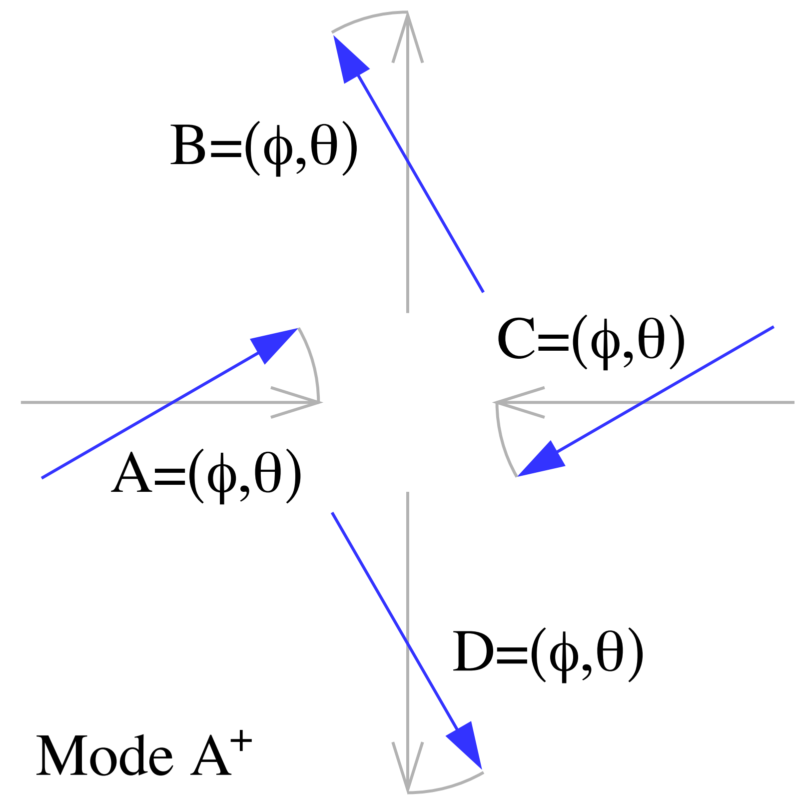

Mode A- has the lowest frequency
at long wavelength.

Mode A+ has the highest frequency
at long wavelength.

There are 4 kinds of modes.

2 are <u>symmetric</u> across the vertex:

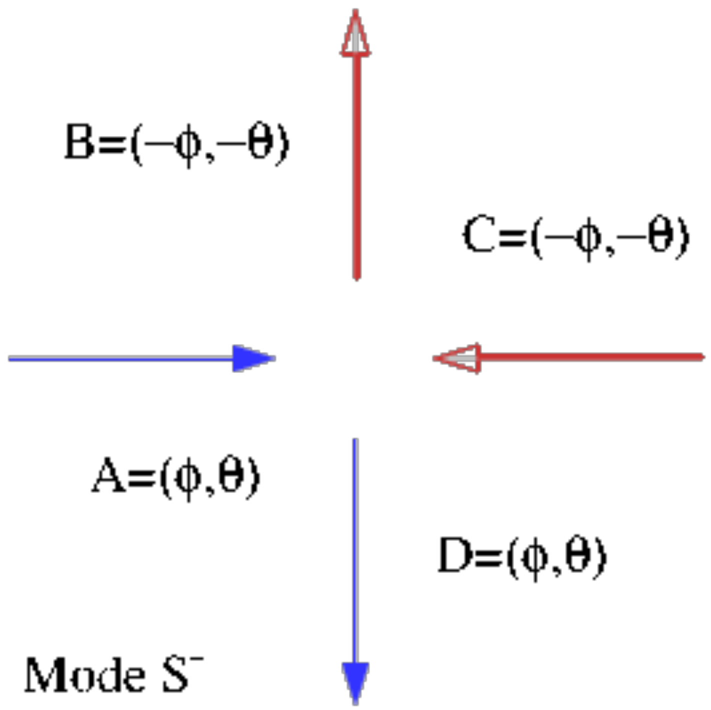

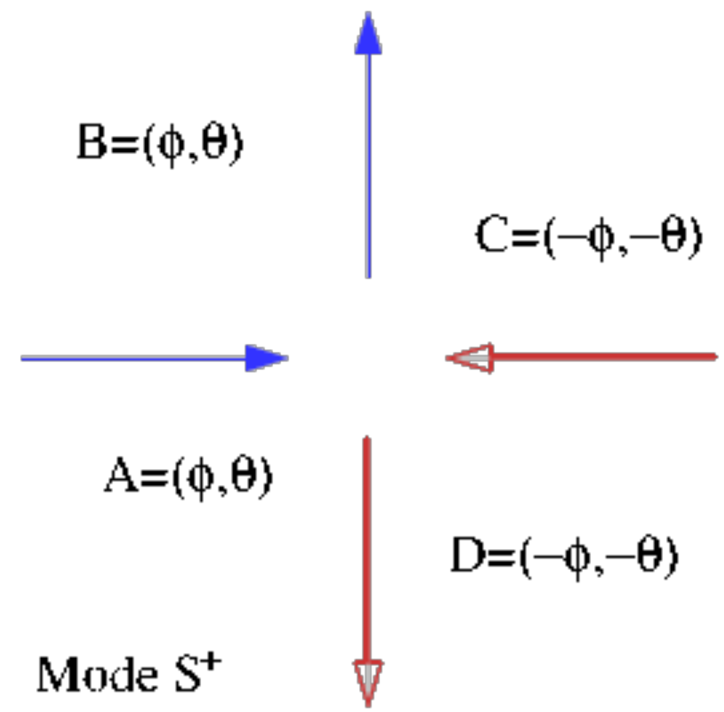

Modes S- and S+ are nearly degenerate at long wavelength.

There are 4 kinds of modes.

2 are symmetric across the vertex:

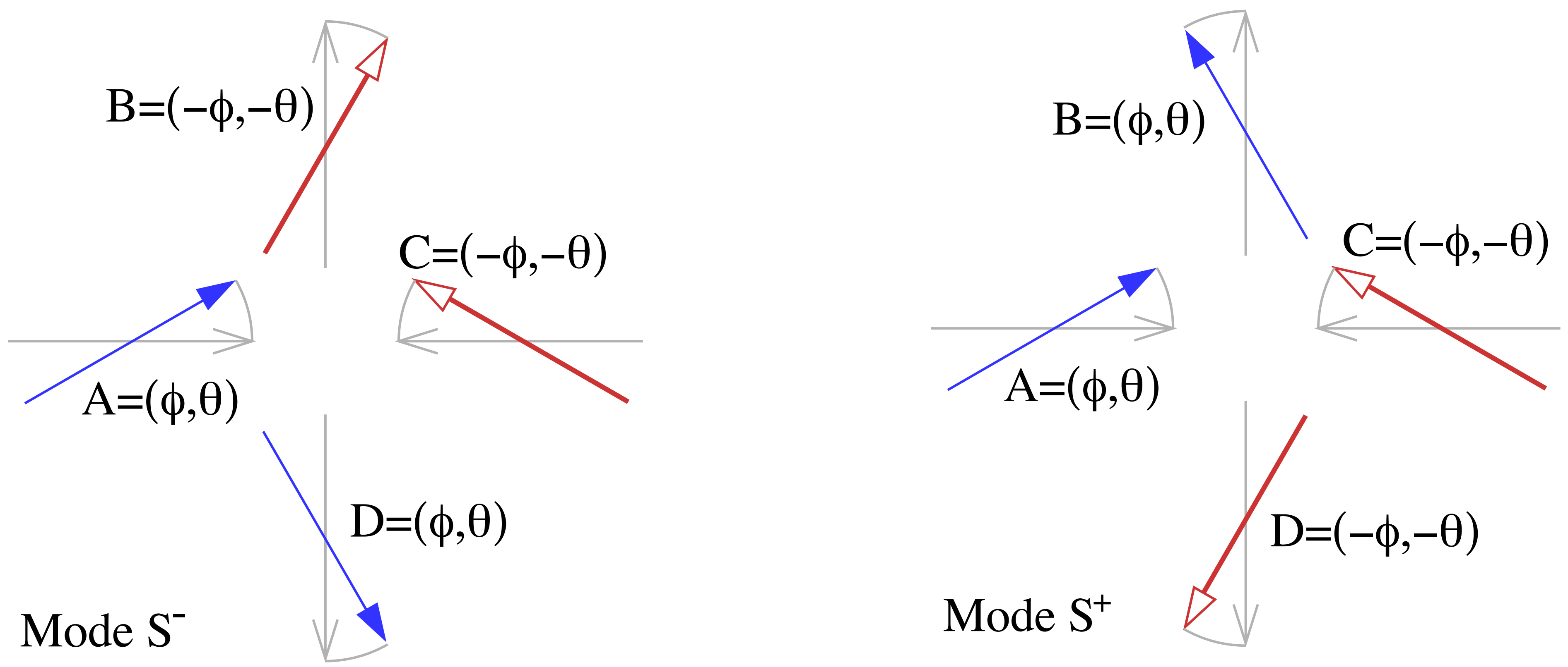

Modes S- and S+ are nearly degenerate at long wavelength.

An excitation spectrum for weak island anisotropy

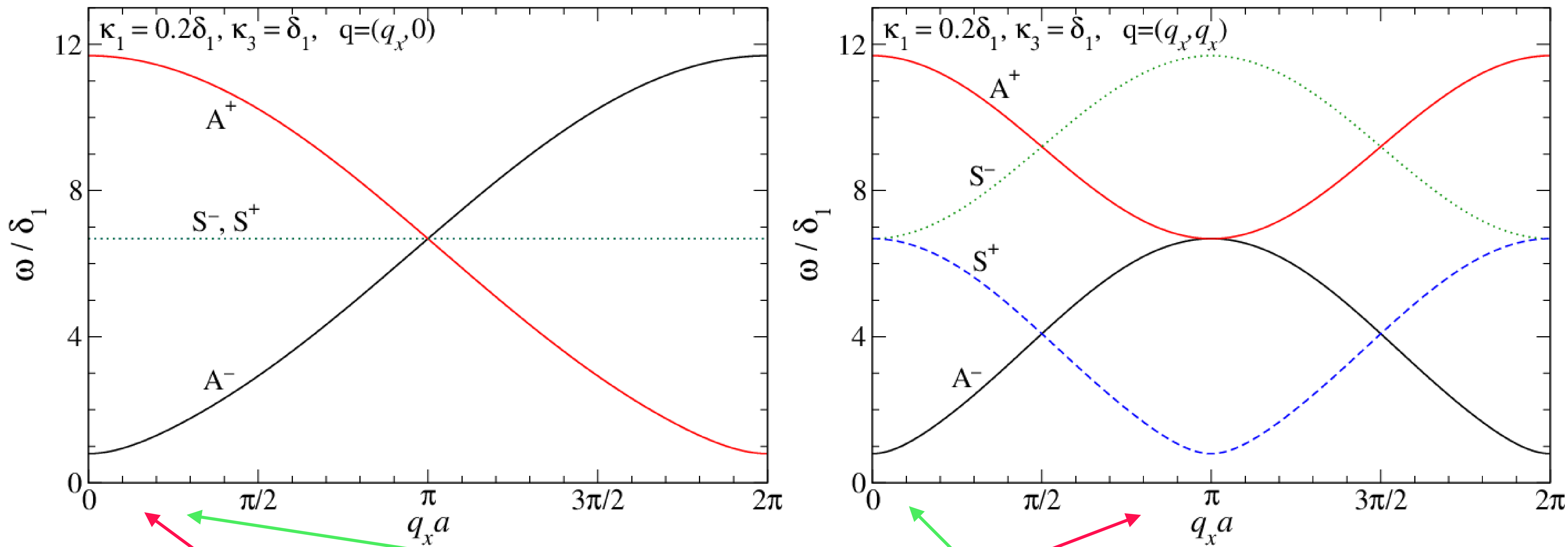

A gap due to island anisotropy

$$\omega_{\mathrm{gap}} = \omega_{\mathrm{A}^-}(0) = \sqrt{\kappa_1(\kappa_{13} + 2\delta_1)}.$$

$A^-(0,0)$, $S^+(\pi/a,\pi/a)$ have lowest energy, are most relevant

But should plot spectrum in 1st Brillouin zone.

The islands' unit cell is tilted at 45 degrees and the islands' lattice constant is *a'*=*a*/sqrt(2).

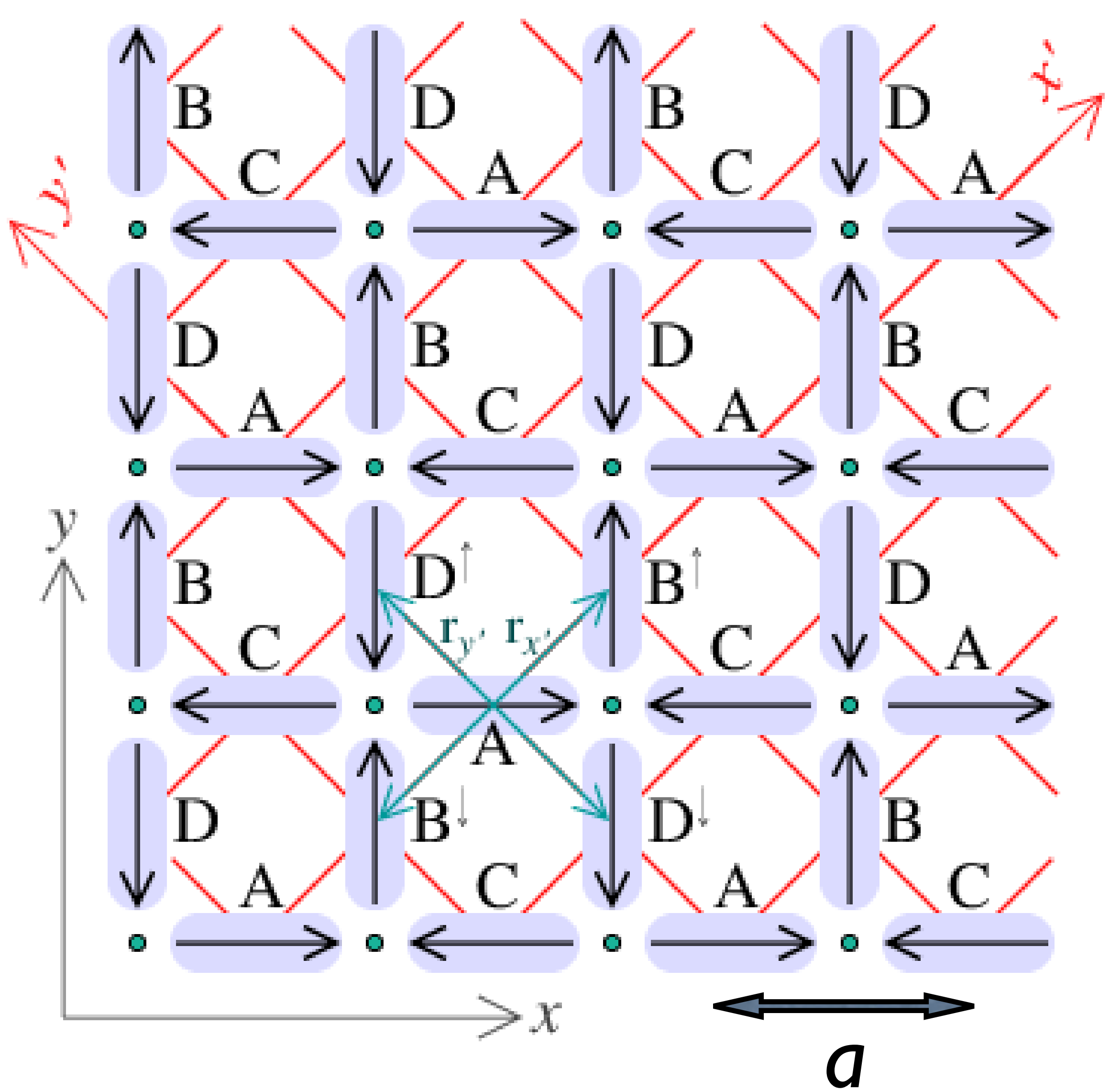

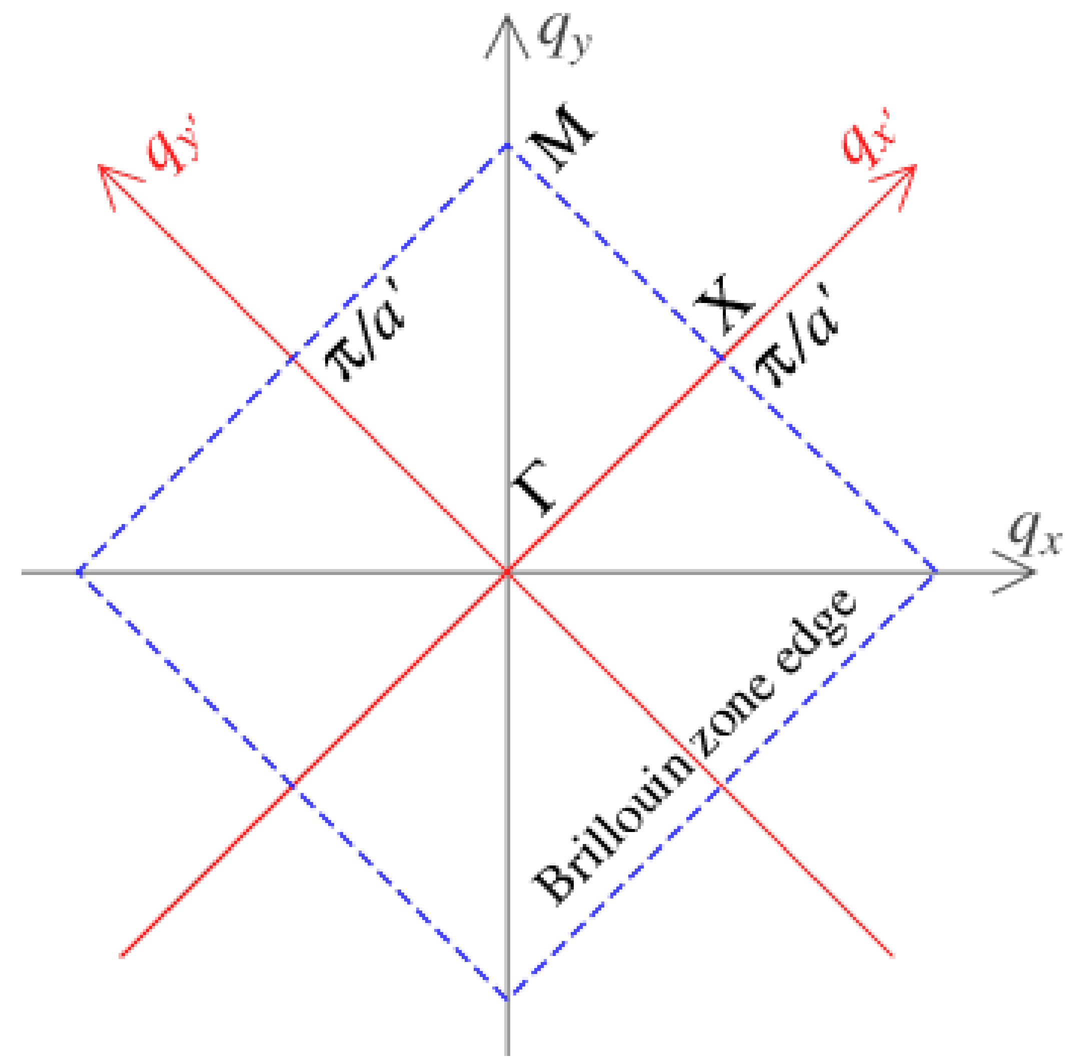

square lattice Brillouin zone.

Plotting spectrum in 1st Brillouin zone.

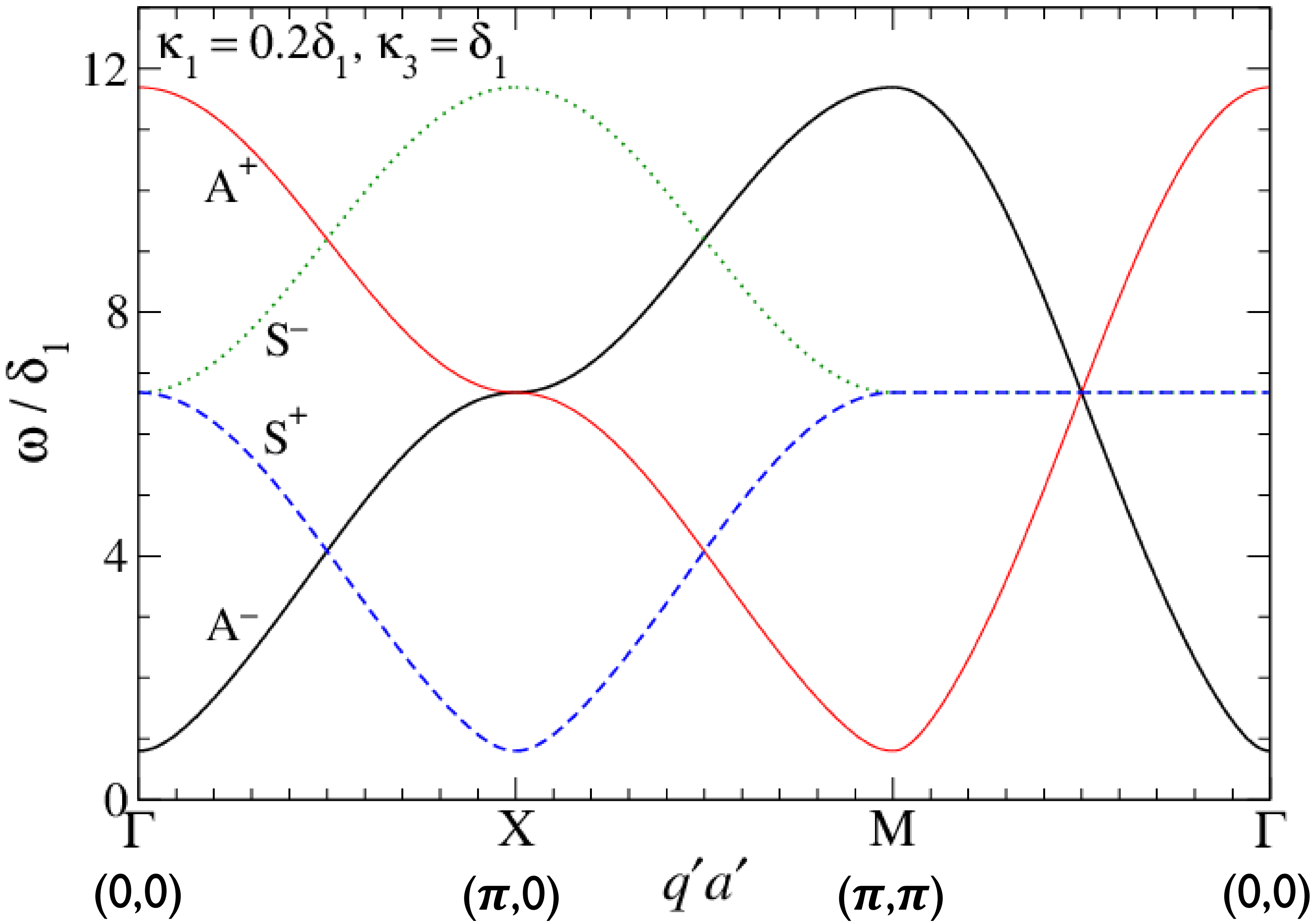

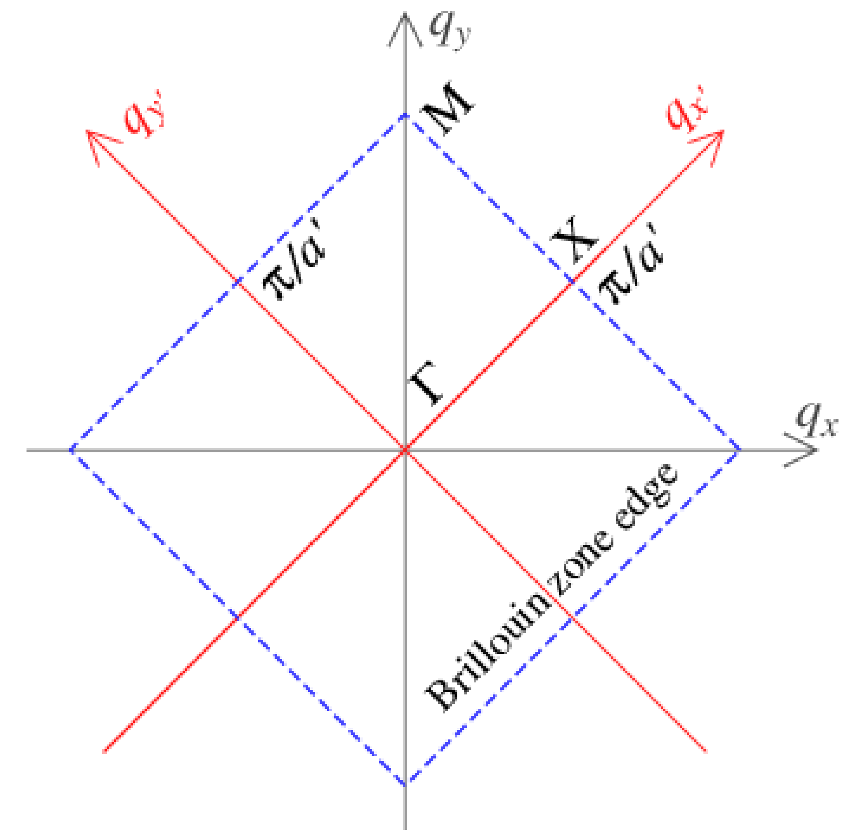

square lattice Brillouin zone.

Future work & improvements

1) Dynamics in remnant state?

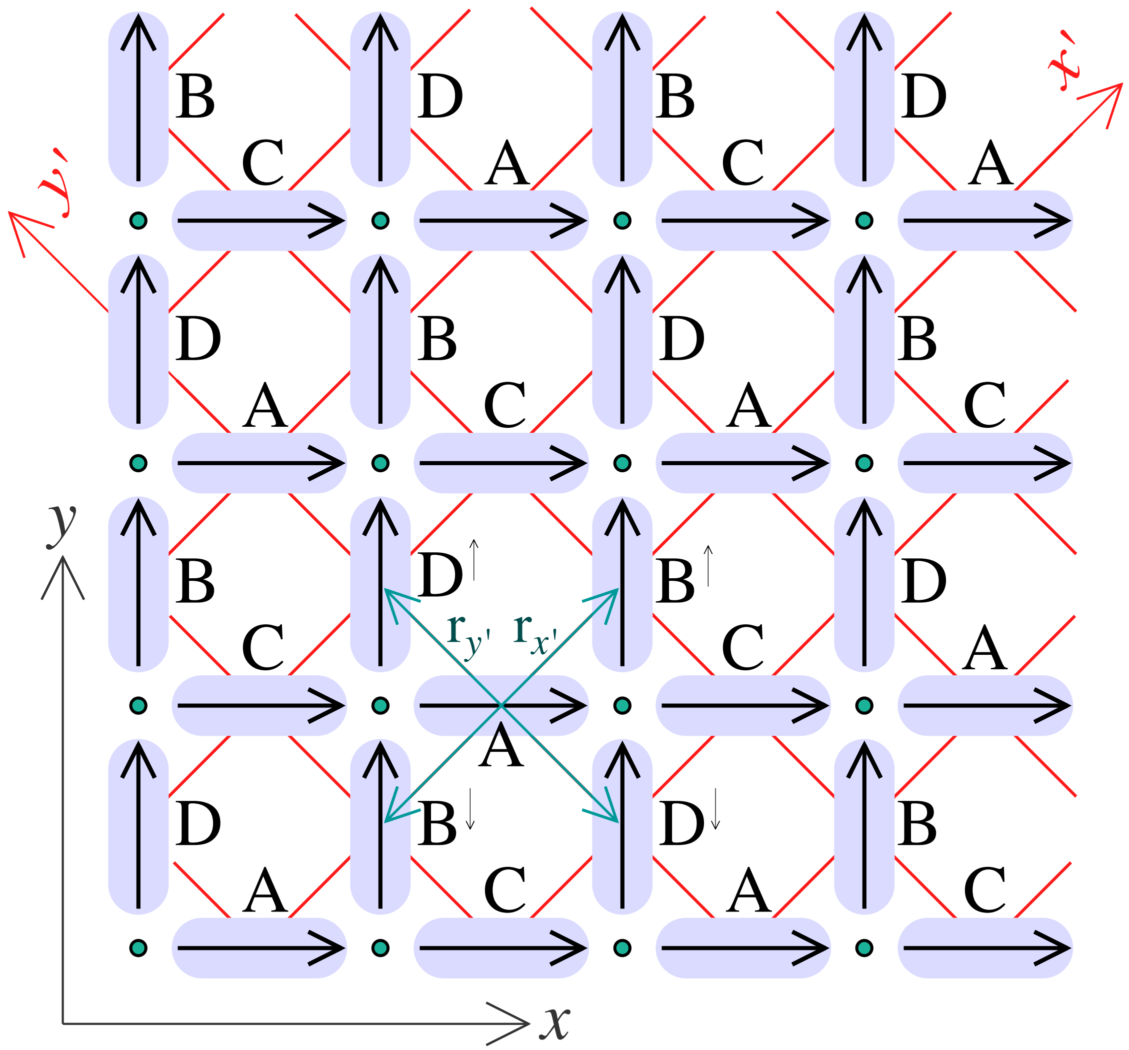

2) Beyond nearest neighbors.
Include long-range dipole interactions.

Summary

Shape anisotropy of magnetic islands has a strong effect on the states.

Anisotropy coefficients for islands used in artificial spin ice are found from the effective potential of the magnetic moment in an island.

A model is developed for spin-ice with continuous dynamics, based on island dipoles which can point in any direction, while constrained by easy-plane and uniaxial anisotropies.

The linearized mode spectrum around a ground state in square ice can be partitioned into symmetric and antisymmetric states; the lowest frequency mode is antisymmetric at long wavelength.

wysin@phys.ksu.edu
www.phys.ksu.edu/personal/wysin